Zika virus noncoding sfRNAs sequester multiple host-derived RNA-binding proteins and modulate mRNA decay and splicing during infection

Received for publication, April 30, 2019, and in revised form, August 19, 2019 Published, Papers in Press, September 13, 2019, DOI 10.1074/jbc.RA119.009129

Daniel Michalski[‡1], **J. Gustavo Ontiveros**[§1], **Joseph Russo**[‡], **Phillida A. Charley**[‡], **John R. Anderson**[‡], **Adam M. Heck**[§2], **Brian J. Geiss**[‡§], and **Jeffrey Wilusz**[‡§3]

From the [‡]*Department of Microbiology, Immunology and Pathology,* [§]*Cell and Molecular Biology Program, Colorado State University, Fort Collins, Colorado 80523*

Edited by Charles E. Samuel

Insect-borne flaviviruses produce a 300–500–base long noncoding RNA, termed subgenomic flavivirus RNA (sfRNA), by stalling the cellular 5′–3′-exoribonuclease 1 (XRN1) via structures located in their 3′ UTRs. In this study, we demonstrate that sfRNA production by Zika virus represses XRN1 analogous to what we have previously shown for other flaviviruses. Using protein–RNA reconstitution and a stringent RNA pulldown assay with human choriocarcinoma (JAR) cells, we demonstrate that the sfRNAs from both dengue type 2 and Zika viruses interact with a common set of 21 RNA-binding proteins that contribute to the regulation of post-transcriptional processes in the cell, including splicing, RNA stability, and translation. We found that four of these sfRNA-interacting host proteins, DEAD-box helicase 6 (DDX6) and enhancer of mRNA decapping 3 (EDC3) (two RNA decay factors), phosphorylated adaptor for RNA export (a regulator of the biogenesis of the splicing machinery), and apolipoprotein B mRNA-editing enzyme catalytic subunit 3C (APOBEC3C, a nucleic acid–editing deaminase), inherently restrict Zika virus infection. Furthermore, we demonstrate that the regulations of cellular mRNA decay and RNA splicing are compromised by Zika virus infection as well as by sfRNA alone. Collectively, these results reveal the large extent to which Zika virus–derived sfRNAs interact with cellular RNA-binding proteins and highlight the potential for widespread dysregulation of post-transcriptional control that likely limits the effective response of these cells to viral infection.

Post-transcriptional regulation of gene expression is a multifaceted and complex cellular process that is critically important for maintaining cellular homeostasis. Therefore, it is not surprising that many aspects of post-transcriptional control are targeted and disrupted by RNA viruses during infection (1). RNA splicing, for instance, is a highly-regulated post-transcriptional process that relies on the proper localization of the spliceosome to avoid aberrant splicing events within the cell. For instance, mutations in the splicing factor SF3B1, a component of the U2 snRNP,[4] induce the usages of alternative splice sites in a subset of targeted host cell genes (2, 3). A recent transcriptome analysis of Zika virus (ZIKV)-infected human neural progenitor cells identified a variety of alternative splicing events in more than 200 different RNAs (4). Precisely how a cytoplasmic virus like ZIKV induces such significant mis-splicing inside the nucleus of infected cells remains unclear.

Other aspects of post-transcriptional control can be impacted by RNA virus infections. The cellular mRNA decay machinery, a fundamental regulator of both the quantity and quality of gene expression, can also be targeted. The decay of most mRNAs generally begins with the deadenylation of the transcript followed by the removal of the 7-methylguanosine 5′ cap. The mono-phosphorylated transcript is then reduced to single nucleotides via the action of the highly-processive cytoplasmic 5′–3′-exoribonuclease XRN1 (5). Considerable evidence has revealed that transcripts of RNA viruses are also actively targeted by the cellular RNA decay machinery (6). Additionally, RNA stability has been shown to regulate the expression of many mRNAs encoding immune mediators (7), further highlighting the critical role of RNA stability during infection. Thus, any perturbations in the ability of the cell to regulate RNA decay can have dramatic effects on the outcome and pathogenesis associated with viral infection.

RNA editing, which can greatly expand the coding capacity of the transcriptome (8), can also have an impact on virus infections. The process consists of the deamination of adenosine to inosine (A-to-I) or cytosine to uracil (C-to-U) and is catalyzed, respectively, by two classes of deaminases: the ADAR and AID/

This work was supported by National Institutes of Health Grants AI123136 and AI130497 (to J. W.) and Grant AI32668 (to B. J. G.). The authors declare that they have no conflicts of interest with the contents of this article. The content is solely the responsibility of the authors and does not necessarily represent the official views of the National Institutes of Health.

This article contains Tables S1–S3.

The MS proteomics data have been deposited to the ProteomeXchange Consortium via the PRIDE partner repository with the dataset identifier accession numbers PXD014933 and 10.6019/PXD014933.

The amino acid sequence of this protein can be accessed through NCBI Protein Database under NCBI accession number GSE135413.

[1] Both authors contributed equally to this work.

[2] Supported in part by National Science Foundation NRT Award 1450032 and by a National Science Foundation GRFP award.

[3] To whom correspondence should be addressed. E-mail: jeffrey.wilusz@colostate.edu.

[4] The abbreviations used are: snRNP, small nuclear ribonucleoprotein; sfRNA, subgenomic flavivirus RNA; PHAX, phosphorylated adaptor for RNA export; ZIKV, Zika virus; DENV, Dengue virus; nt, nucleotide; dd, digital droplet; hpi, hours post-infection; GAPDH, glyceraldehyde-3-phosphate dehydrogenase; RBP, RNA-binding protein; PMSF, phenylmethylsulfonyl fluoride; KINV, Kunjin virus; 4SU, 4-thiouridine; DM, double mutant; m.o.i., multiplicity of infection; HCV, hepatitis C virus; xrRNA, XRN1-resistant RNA.

APOBEC proteins (9). RNA-editing activity has been reported in APOBEC1, APOBEC3A (10), and APOBEC3G (11), but not for other members of the family to date. APOBEC3G has been implicated as a major restriction factor for retroviruses (12). There is also evidence that APOBEC3G has antiviral functions against hepatitis C virus (HCV), a member of the Flaviviridae (13, 14). The goal of this study was to expand upon this previous work and to assess in an unbiased fashion the interaction between a major noncoding transcript made by all insect-borne flaviviruses and the cellular post-transcriptional control machinery.

Flaviviruses are single-stranded positive-sense RNA viruses that are responsible for a variety of significant human diseases. It has been estimated that ~2/3rd of the world population is at risk for infection by one or more of the 35 flaviviruses known to cause human disease (15). The most well-known members of this virus family are arboviruses: Dengue viruses (DENV), West Nile virus, Japanese encephalitis virus, and ZIKV, which utilize arthropod vectors as a key part of their transmission cycles. The flavivirus genomic RNA is typically between 10 and 11 kb and contains a single large polyprotein-encoding open reading frame (ORF) flanked by untranslated regions (UTRs). A key characteristic common to all arthropod-borne flavivirus infections tested to date is the generation and accumulation of a small 300–500-base subgenomic flavivirus RNA (sfRNA), which represents the majority of the 3′ UTR of the viral genomic RNA (16). Interestingly, flaviviral sfRNAs are not generated using a subgenomic promoter but rather by stalling of the cellular 5′–3′-exoribonuclease XRN1 as it attempts to degrade viral positive-sense transcripts inside infected cells (17–21). All insect-borne flaviviruses tested to date contain a knot-like three-helix junction structure in the proximal portion of their 3′ UTR that stalls XRN1. The activity of XRN1 is also repressed by sfRNA generation in DENV and Kunjin virus (KUNV) infections, presumably due to slow release of the enzyme from the knot-like RNA structure (22, 23). The sfRNA-mediated repression of XRN1 apparently feeds back and also shuts down upstream functions of the decay pathway (6, 24). This results in stabilization of cellular mRNAs and dysregulation of their expression, which can be particularly dramatic for short-lived mRNAs (*e.g.* cytokines and innate immune factors). In addition, the high levels of sfRNA that are generated can serve as a sponge for cellular RNA-binding proteins and repress their function. To date, targeted functions include interferon, innate immunity, and RNAi (25–32).

Zika virus (ZIKV) is a flavivirus that was discovered in 1947 in the forests of Uganda, and its transmission is mediated primarily by *Aeges aegypti* and possibly *Aedes albopictus* mosquitoes (33). Most ZIKV infections are asymptomatic, and those that do show symptoms typically have mild fever, rash, arthralgia, and/or conjunctivitis (34). Notably, however, ZIKV infection during pregnancy can lead to fetal loss, microencephaly, and brain/eye abnormalities. ZIKV causes a spectrum of neurological damage in the developing fetus and can lead to Guillain-Barre syndrome, a condition in which the immune system damages neuronal cells. The mechanisms underlying flavivirus-associated pathogenesis are still largely unclear (35). Thus, it is very important to understand how these viruses interface with host-cell factors. The purpose of this study was to catalog the major cellular RNA-binding proteins that interact with the sfRNA generated during ZIKV infection and to provide foundational data for potential molecular mechanisms of sfRNA-associated cytopathology.

In this study, we show that ZIKV infection in human cells leads to the accumulation of two sfRNA species that are associated with an increase in both the abundance and stability of normally short-lived host cellular mRNAs, mirroring previous reports of other sfRNA-generating members of the Flaviviridae. ZIKV sfRNA selectively associated with over 20 RNA-binding proteins that affect a multitude of post-transcriptional cellular processes. Two of these factors, DDX6 and EDC3, are known RNA-decay factors that represent viral restriction factors. Likewise, we found that sfRNA-associated host cell splicing factors PHAX and SF3B1 were also viral restriction factors. Both SF3B1-mediated RNA splicing and DDX6/EDC3-mediated RNA decay were shown to be significantly dysregulated during ZIKV infection. Thus, the generation of sfRNA during ZIKV infection appears to have two major functional roles inside the host cell: 1) XRN1 repression and the resulting stabilization of normally short-lived host mRNAs, and 2) that of a protein sponge for host RNA-binding proteins to disrupt aspects of cellular gene expression that may limit the ability of the cell to effectively respond to the viral infection.

Results

Accumulation of sfRNAs in ZIKV-infected cells is associated with a significant increase in the abundance and stability of normally short-lived host cell mRNAs

A number of previous studies on arthropod-borne members of the Flaviviridae indicate that the major 5′–3′-cytoplasmic exoribonuclease XRN1 stalls on specific structures near the proximal portion of the viral 3′ UTR sequence (17, 19, 21, 22, 36). This gives rise to a stable decay intermediate known as sfRNA. The accumulation of these sfRNAs in KUNV and DENV-2 infections has been shown to repress XRN1 function and dysregulate host cell mRNA stability (22). Being a member of the Flaviviridae, we hypothesized that ZIKV infection would also result in significant sfRNA accumulation and dysregulation of normally short-lived host mRNAs. To test this hypothesis, we performed a time course of ZIKV infection in human choriocarcinoma cells (JAR cells). As seen in Fig. 1*A*, sfRNAs of 415 and 330 nts accumulated to high levels in ZIKV-infected JAR cells between 48 and 72 h post infection. To determine the impact of ZIKV infection on cellular mRNA half-lives, infected cells were metabolically labeled with 4-thiouridine (4SU) for 60 min. Purified total RNA was then fractionated into unlabeled "pre-existing" and 4SU-labeled "nascent" RNA populations and subjected to quantitative ddRT-PCR analysis using primers to the FOS and JUN cellular mRNAs. As seen in Fig. 1*B*, both the abundance and stability of the FOS and JUN mRNAs were significantly increased at 72 hpi. Thus, we conclude that the generation of ZIKV sfRNA, as has been previously shown for two other insect-borne flaviviruses (22), is associated with a significant increase in the abundance and stability of short-lived cellular mRNAs.

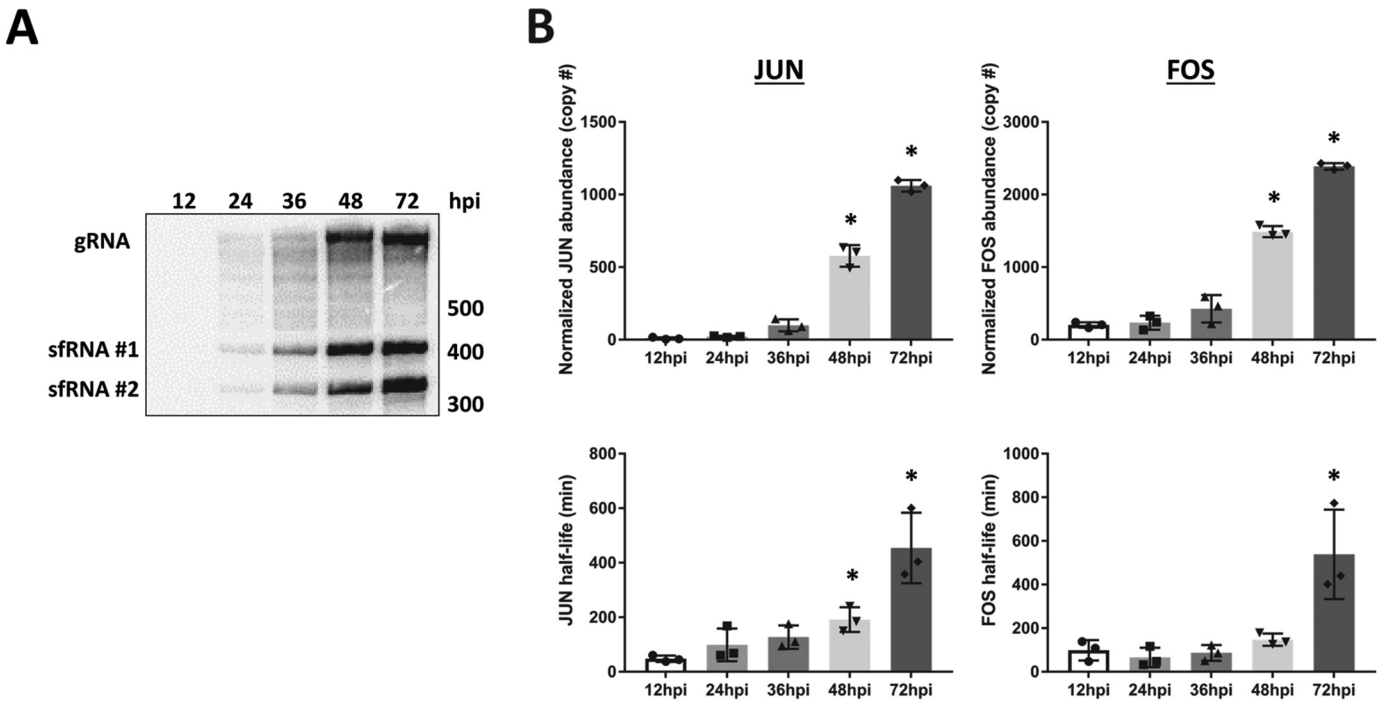

Figure 1. Accumulation of two sfRNA decay intermediates in ZIKV infection coincides with an increase in both the stability and abundance of normally short-lived host cell mRNAs. *A,* representative Northern blotting of total RNA from ZIKV-infected JAR cells isolated at the indicated time post-infection. RNAs were separated on a 5% denaturing acrylamide gel, probed with a radiolabeled probe complementary to the first 77 nt of the ZIKV 3′-UTR, and visualized by phosphorimaging. The position of size markers on the gel is indicated on the *right*. *B,* newly synthesized RNAs from mock-infected or ZIKV-infected JAR cells were metabolically labeled with 4SU at the indicated times post-infection. RNAs were separated into unlabeled and 4SU-labeled populations and subjected to quantitative ddRT-PCR analysis using primers to the *FOS* and *JUN* cellular mRNAs. The *top graphs* depict the abundance changes of the indicated mRNA relative to mock-infected cells, and the *bottom graphs* depict the mRNA stability relative to infected cells as determined by half-life calculations. Results are shown as the mean ± S.D. determined from three independent infections. Significance was determined using a Student's *t* test with * = $p \leq 0.05$.

Next, we used a biochemical reconstitution approach to provide direct evidence that the stalling of XRN1 on established structures in the ZIKV 3′ UTR represses enzymatic activity. As seen in Fig. 2*A*, the incubation of purified recombinant XRN1 with RNAs containing the WT ZIKV 3′ UTR resulted in the generation of two sfRNA species consistent in size with the two sfRNAs generated in infected cells (Fig. 1*A*). Mutations that were shown previously to disrupt the first XRN1-resistant (xr)RNA structure (MUT1) or second xrRNA structure (MUT2) (36) showed dramatic reductions in the generation of the respective sfRNA species (Fig. 2*A*, *lanes MUT1* and *MUT2*). RNAs containing mutations in both ZIKV xrRNA structures (double mutant (*DM lanes*)) resulted in the complete loss of XRN1 stalling and no generation of sfRNA species. Similar results were obtained using human (HeLa) or mosquito (C6/36) cytoplasmic extracts under conditions that promote XRN1 activity (Fig. 2*A*, *lower panels*).

XRN1 stalling in the 3′ UTR of two other flaviviruses tested to date (DENV and KUNV) also results in a reversible repression of enzymatic activity presumably due to the slow release of the stalled enzyme from the RNA substrate (22–23). To determine whether the ZIKV 3′ UTR can also repress XRN1 activity, cold competitor RNAs containing sequences from control plasmid, DENV-2 3′ UTR, ZIKV-3′ UTR, or the ZIKV double mutant (DM) 3′ UTR (that cannot stall XRN1/form sfRNAs) were generated and incubated along with a radiolabeled reporter RNA and XRN1. RNA reaction products were analyzed on an acrylamide gel at various time points post-XRN1 incubation to assess relative exonuclease activity in the presence of each competitor RNA. As seen in Fig. 2*B*, the inclusion of a 20-fold molar excess of monophosphorylated unlabeled DENV competitor RNA relative to radiolabeled RNA substrate effectively reduced XRN1 activity during the time course. Interestingly, the ZIKV 3′ UTR competitor RNA also repressed XRN1 to a similar level as DENV, whereas neither the control RNA nor the ZIKV double sfRNA mutant (DM) RNA affected XRN1 activity (Fig. 2*B*). Therefore, we conclude that the ZIKV 3′ UTR, similar to other flavivirus 3′ UTRs, can both stall and repress the cellular XRN1 enzyme.

ZIKV and DENV sfRNAs bind to a common set of RNA-binding proteins that influence an array of post-transcriptional processes

The stalling of XRN1 by flavivirus xrRNA structures results in the generation of copious amounts of sfRNA in infected cells. These sfRNAs may serve as a sponge for a number of cellular RNA-binding proteins that may have a significant influence on cellular physiology and host–virus interactions. Previous work has indeed indicated that flavivirus sfRNAs can interact with proteins involved in RNAi, innate immunity, interferon responses, and translational regulation (25–32). To build upon these studies, we performed RNA pulldown assays using either a control RNA, DENV-2 sfRNA, or ZIKV sfRNA in HeLa cytoplasmic extracts under relatively stringent conditions followed

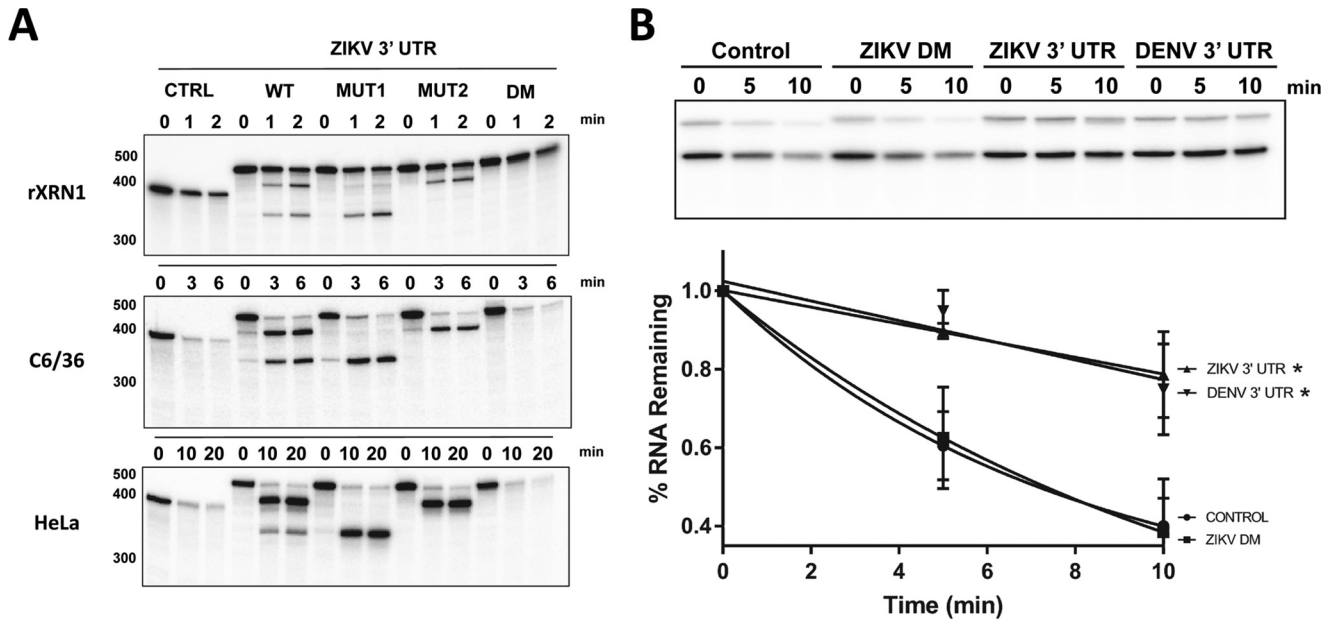

Figure 2. ZIKV 3′-UTR stalls and represses the activity of the host cell 5′–3′-exoribonuclease XRN1. *A,* radiolabeled, 5′-monophosphorylated control (*CTRL*) RNA or RNAs containing the intact ZIKV 3′-UTR or with mutations that debilitate the first (*MUT1*), second (*MUT2*), or both (*DM*) structures that lead to the formation of sfRNAs in cells were incubated with either recombinant XRN1, C6/36 mosquito cytoplasmic extract, or HeLa cytoplasmic extract for the indicated amount of time. Reaction products were analyzed on a 5% denaturing acrylamide gel and quantified by phosphorimaging. The position of size markers is indicated on the *left*. *B*, 61 base-radiolabeled reporter RNA derived from pGEM4 was incubated with XRN1 (derived from HeLa extract) in the presence of a 20× excess of a cold competitor RNA derived from either pGEM4 (*control RNA lanes*), the DENV-2 3′ UTR (*DENV 3′ UTR lanes*), the ZIKV 3′ UTR (*ZIKV 3′ UTR lanes*), or the ZIKV 3′ UTR containing mutations that prohibit sfRNA formation (*ZIKV DM lanes*) for the times indicated. Radiolabeled reaction products derived from XRN1 acting on the reporter RNA were resolved on a 5% acrylamide gel containing urea and visualized by phosphorimaging. Gels from three independent experiments were quantified, and results are shown graphically in the *lower panel*. The *asterisk* represents a p value of <0.001 at both time points for viral 3′ UTR/fragments compared with the control as determined using Tukey's multiple comparisons test as a post hoc test. The gel in the *top portion* is representative data from these same experiments.

by the identification and analysis of associated proteins by MS. Peptide thresholds (95%) were set to achieve a negligible false discovery rate, and protein identifications were accepted if they could be established at greater than 95.0% probability and contained at least two identified peptides. Using these parameters, the MS analysis revealed a total of 222 proteins associated with all three RNAs. As seen in Fig. 3*A* (and Tables S1–S3), 28 proteins specifically associated with both the DENV-2 and ZIKV sfRNA, but not with the size-matched control RNA. The direct pulldown of a representative set of four of these proteins from cytoplasmic extracts by biotinylated flavivirus 3′ UTRs is shown in Fig. 3*D* for further validation. Because these proteins interacted with both flavivirus sfRNAs, they are more likely to represent biologically relevant interactions and thus were the focus of subsequent analyses. As seen in Fig. 3*B*, 21 of these proteins were associated with RNA-related biological processes. To validate the interactions, we chose five representative proteins involved in RNA decay, splicing, or editing and performed immunoprecipitation experiments from ZIKV-infected cell extracts. As seen in Fig. 3*C*, all five of these proteins co-precipitated virus-made sfRNA significantly above the IgG control background. Not surprisingly, given that the sfRNAs represent the 3′ UTR of the viral genomic RNA, full-length viral RNAs are also co-precipitated with the proteins (data not shown). Therefore, we conclude that both DENV-2 and ZIKV sfRNAs interact with these five proteins in a specific fashion during infection and may sequester them in an effort to dysregulate post-transcriptional processes.

ZIKV sfRNA sequesters two viral restriction factors that are involved in aspects of cellular RNA decay

We next set out to determine the relevance of these five sfRNA-binding proteins to ZIKV infections. We first focused on two proteins (DDX6 and EDC3) involved in aspects of RNA decay. DDX6 is a helicase that plays a role in translation suppression and RNA decay (37), and EDC3 is an enhancer of RNA decapping (38). We used siRNAs to effectively knock down these proteins in HEK293 cells (Fig. 4*A*). As seen in Fig. 4*B*, reduction of the level of either DDX6 or EDC3 protein resulted in a significant increase in the abundance of ZIKV RNAs in infected cells. In the case of DDX6 knockdown, this resulted in a significant increase in mature virus released from cells (Fig. 4*C*). Knockdown of EDC3 did not result in a substantial increase in infectious virus released from cells (Fig. 4*C*), perhaps due to the smaller effects that the knockdown had on ZIKV RNA abundance in infected cells relative to DDX6 knockdown. In addition, the sfRNA naturally present in the infection may already be effectively sequestering a great deal of the EDC3 protein, thereby muting the effects of knocking down the factor during infection. To confirm and complement these results, we also overexpressed DDX6 or EDC3 in HEK293 cells (Fig. 4*D*) and determined the effect on ZIKV RNA and virus production. Overexpression of either DDX6 or EDC3 significantly reduced both ZIKA RNA abundance (Fig. 4*E*) and virus particle production (Fig. 4*F*). Therefore, we conclude that both DDX6 and EDC3 cellular proteins are viral restriction factors

A

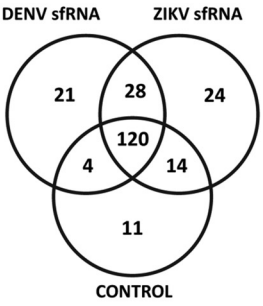

B

BIOLOGICAL PROCESS:	sfRNA-BINDING PROTEINS:
RNA Decay	DDX6, EDC3
RNA Splicing	PHAX, SF3B1, SF3B2,PRPF19, PPIH, NMP1, PCBP2, RTCB, HNRNPK, HNRNPF, HNRNPH1
Nucleic Acid Editing	APOBEC3C
Translation/Ribosome Factors	LSM14B, RPL22, RPL17, RPL7a, EEF1A1, TDRD3, BRIX1

C

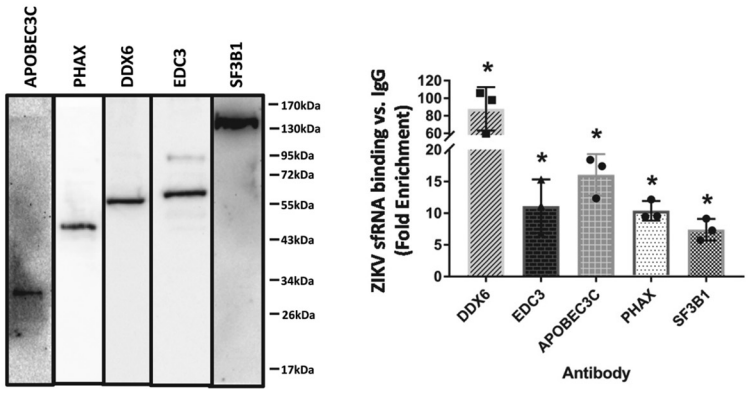

D

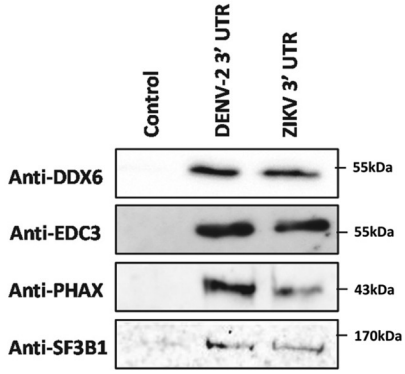

Figure 3. ZIKV and DENV-2 sfRNAs interact with a common set of 28 proteins that impact a variety of aspects of cellular post-transcriptional gene regulation. *A,* biotinylated RNAs containing the DENV-2 3′ UTR, ZIKV 3′ UTR, or a size-matched control transcript were incubated with HeLa cytoplasmic extracts. Proteins that co-purified with the RNAs on streptavidin beads were identified by MS. *A,* Venn diagram depicting the number and commonality of human host-cell RNA-binding proteins identified via MS for each RNA. *B* shows a grouping of proteins that bound to both the ZIKV 3′-UTR and DENV 3′-UTR into the post-transcriptional process associated with each protein. *C,* ZIKV sfRNA directly binds to a variety of cellular RNA-binding proteins in infected cells. *Left side*, Western blotting documenting the specificity of the antibodies used in the panel. *Right side,* 293T cells were infected with ZIKV for 48 h; formaldehyde was added to the cultures to stabilize RNA–protein complexes, and total cell extracts were prepared. Antibodies to RNA decay factors DDX6 and EDC3, RNA-splicing factors PHAX and SF3B1, and the RNA-editing factor APOBEC3C or normal rabbit IgG were added to immunoprecipitated RNA–protein complexes. Co-purifying RNAs were analyzed by digital droplet RT-PCR using primers to the Zika virus sfRNA/3′-UTR. The abundance of ZIKV RNA co-precipitated using the various antibodies was determined relative to the amount pulled down in the normal rabbit IgG control. Results are shown as the average ± S.D. from three independent infections. *D,* biotinylated RNAs containing the 3′ UTRs of DENV-2 or ZIKV, as well as a size-matched control RNA, were incubated with cytoplasmic extracts. Associated proteins were eluted, separated on a 10% SDS-acrylamide gel, and probed with the antibodies indicated on the *left* by Western blotting.

whose activity may be partially suppressed by interactions with sfRNA during ZIKV infection.

ZIKV sfRNA sequesters restriction factors that are involved in RNA splicing and nucleic acid editing

We next focused on determining the effect of two proteins involved in splicing (SF3B1 and PHAX) and one nucleic acid deaminase (APOBEC3C). SF3B1 is part of the U2 snRNP complex involved in the basic cellular splicing machinery (2), and PHAX is involved in U small nuclear RNA nuclear export for its maturation in the cytoplasm (39). APOBEC3C is a cytidine deaminase that is localized to both the nucleus and cytoplasm and has been implicated in deamination of C to T residues in DNA (40). A close relative of this protein, APOBEC1, has been implicated in the post-transcriptional editing of C residues to U in RNA (40). We obtained siRNAs to target the expression of each of these proteins and obtained successful knockdown (Fig. 5*A*). Unfortunately, knockdown of SF3B1 in our experiments resulted in cells with poor growth characteristics and thus were excluded from further analyses. As seen in Fig. 5, *B* and *C*, knockdown of either PHAX or APOBEC3C resulted in a significant increase in ZIKV viral RNA in infected cells as well as an increase in virus production. In complementary experiments, overexpression of either PHAX or APOBEC3C (Fig. 5*D*) resulted in a significant decrease in ZIKV RNA abundance (Fig. 5*E*) as well as virus particle production (Fig. 5*F*). Based on these results, we conclude that both the splicing-associated factor PHAX and the nucleic acid deaminase APOBEC3C are viral restriction factors whose activity may be partially suppressed by interaction with sfRNA during ZIKV infection.

Nuclear splicing is significantly disrupted during ZIKV infection

We next wanted to establish whether nuclear splicing that is mediated by factors that interact with ZIKV sfRNA is indeed dysregulated as we would predict. The splicing of *SRSF7*, a gene that encodes a member of the family of SR proteins, was previously shown to be a direct target of SF3B1 (2, 3), a splicing factor that interacts with ZIKV sfRNA (Fig. 3). Thus, we chose to evaluate the splicing of exons 2–8 of SRSF7 in HEK293T cells during ZIKV infection (Fig. 6*A*). In uninfected cells, exons 2–8 are consecutively joined together, as reported previously (Fig. 6*B*, *lane C*) (2, 3). However, 48 h after infection with ZIKV (when a substantial amount of sfRNA has accumulated in the cell (Fig. 1*A*)), a number of aberrantly spliced mRNA products appear (Fig. 6*B*, *lane ZIKV*). Sequencing of these two aberrantly spliced products indicated that they resulted from the use of cryptic 5′ and 3′ splice sites. Aberrantly spliced product #1 had a truncated exon 3, and the retention of a portion of intron sequence attached to exon 4 (Fig. 6*C*, *top*). Aberrantly spliced product #2 resulted from skipping of exon 3, and the

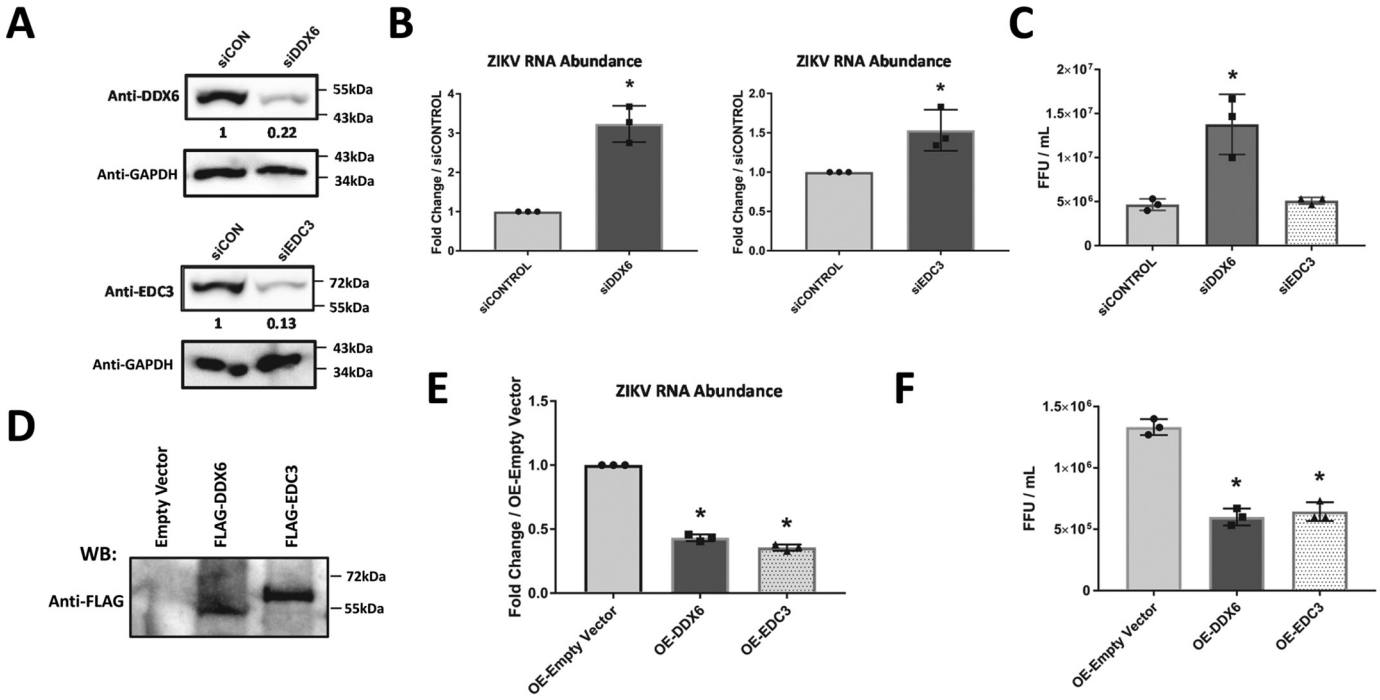

Figure 4. Host RNA decay factors DDX6 and EDC3 function to inhibit ZIKV replication and limit infectious virus production. *A,* representative Western blotting depicting endogenous DDX6 and EDC3 protein levels in ZIKV-infected 293T cells treated with either a control siRNA, a siRNA targeting DDX6, or a siRNA targeting EDC3. *B,* effects of siRNA-mediated knockdown of RNA decay factors DDX6 and EDC3 on ZIKV sfRNA production in infected 293T cells compared with siRNA Control knockdown is as determined via ddPCR. The average fold-change ± S.D. from three independent infections is shown. *C,* focus forming assay: Vero cells infected with the viral supernatant from the siRNA knockdown samples described in *B*. The average number of foci per ml ± S.D. from three independent infections is depicted. *D–F,* effects of overexpressing 3×FLAG-tagged DDX6 and EDC3 from a transfected plasmid in 293T cells during ZIKV infection. The average fold-change ± S.D. from three independent infections is represented on the *graph*. *D,* representative Western blotting showing 3×FLAG-tagged overexpression of DDX6 and EDC3 in 293T cells. Total protein from cells that were transfected as indicated above the *three lanes* was electrophoresed on a 10% SDS-acrylamide gel, blotted, and probed with anti-FLAG antibody. *E,* effects of overexpressing 3×FLAG-tagged DDX6 and EDC3 on ZIKV sfRNA production in infected 293T cells compared with an empty control vector as determined via ddPCR. The average fold-change ± S.D. was from three independent infections. *F,* focus-forming assay: Vero cells infected with the viral supernatant from the overexpression samples described in *D*. The average number of foci per ml ± S.D. from three independent infections is depicted. Significance in *B, C, E,* and *F* was determined by *t* test with * = $p \leq 0.05$.

retention of a portion of intron sequence attached to exon 4 (Fig. 6*C*, *bottom*). Therefore, we conclude that nuclear splicing is dysregulated in ZIKV infection in a manner that would be consistent with sfRNA-mediated sponging of splicing factors.

Next, we investigated potential changes in RNA editing that could be associated with the sponging of APOBEC3C by ZIKV sfRNA. Global RNA-Seq experiments comparing early (12 hpi) and late (72 hpi) times post-infection failed to demonstrate any difference in RNA editing as discerned from the analysis of base conversion ratios (*e.g.* 0.22% adenosine to guanine (A to G) at 12 hpi *versus* 0.23% at 72 hpi with all other base changes at comparable levels). Additionally, sequencing of the 3′ UTR from 10 ZIKV isolates obtained from cells with overexpressed levels of APOBEC3C failed to show any evidence of increased RNA editing compared with control cells (no mutations were found in any of the isolates). Thus, we conclude that the interaction of ZIKV sfRNA with APOBEC3C does not appear to alter C→U RNA editing in infected cells. APOPBEC3C may be playing other roles (41), including altering protein–protein interactions or DNA editing, which may impact viral replication efficiency. Efforts to elucidate the role of APOBEC3C during ZIKV will be addressed in future studies.

Flavivirus sfRNA alone is sufficient to cause changes in cellular mRNA abundance and splicing

Finally, we wished to determine whether flavivirus sfRNA alone was sufficient to mediate the changes in cellular RNA stability and processing noted above. Therefore, in the absence of viral infection we transfected RNAs containing either the DENV-2 or ZIKV 3′ UTR, as well as a size-matched control RNA, into HEK293T cells and evaluated the impact of the RNA on cellular mRNA abundance and splicing. As seen in Fig. 7*A*, both the DENV-2 as well as ZIKV sfRNAs on their own mediated a significant increase in the abundance of the normally short-lived *JUN* and *FOS* mRNAs. This effect is similar to the pattern of increased *JUN* and FOS mRNA abundance observed during viral infection (Fig. 1*B*) (22). As seen in Fig. 7*B*, splicing of the SRSF7 was also specifically impacted by transfection of sfRNA alone, generating the aberrantly spliced product #2 that was observed in viral infection (Fig. 6*B*). Therefore, these data indicate that sfRNA is directly dysregulating cellular gene expression at the post-transcriptional level.

Discussion

This study provides several novel insights into the function of ZIKV sfRNA. First, the generation of ZIKV sfRNA represses XRN1 activity similar to several other viral RNA structures that

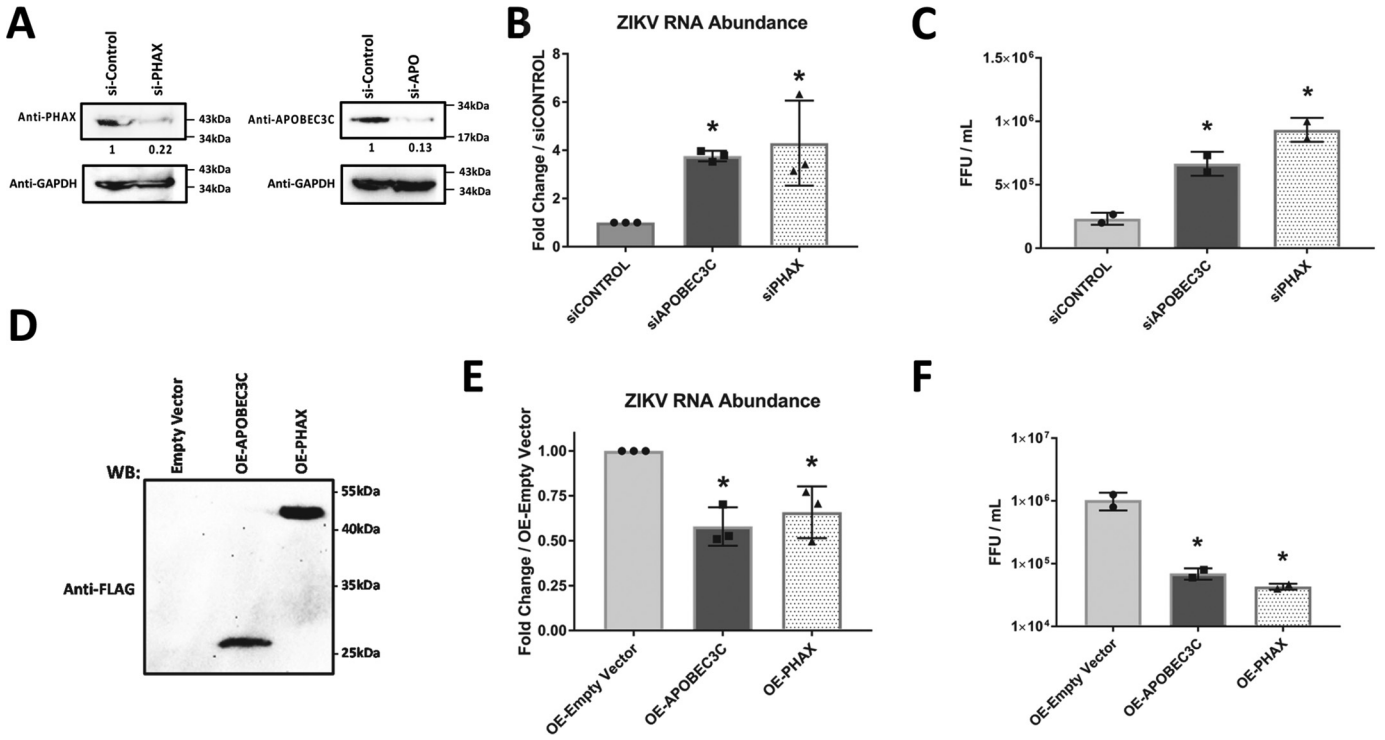

Figure 5. Splicing factor PHAX and the nucleic acid deaminase APOBEC3C are restriction factors for ZIKV replication. *A,* siRNAs targeting PHAX or APOBEC3C or a nonspecific control siRNA were transfected into HEK293 cells. The levels of the indicated proteins were determined by Western blotting. The *blots* shown are representative of three independent experiments. *B,* relative levels of ZIKV RNA in cells transfected with either control, PHAX, or APOBEC3C targeting siRNAs were determined at 48 hpi. The data are presented as fold-change relative to the ZIKV levels present in cells transfected with the control siRNA. *C,* focus-forming assay: Vero cells infected with the viral supernatant from the siRNA knockdown samples described in *B*. The average number of foci per ml ± S.D. from three independent infections is depicted. *D,* FLAG-tagged versions of APOBEC3C and PHAX were constructed on expression vectors and transfected into HEK293 cells. The levels of the indicated proteins were determined by Western blotting. *E,* relative levels of ZIKV RNA in cells transfected with either empty vector, FLAG-PHAX, or FLAG-APOBEC3C expression plasmids were determined at 48 hpi. The data are presented as fold-change relative to the ZIKV levels present in cells transfected with the empty vector. *F,* focus-forming assay: Vero cells infected with the viral supernatant from the overexpression samples described in *D*. The average number of foci per ml ± S.D. is depicted. All data are the results of three independent biological experiments. * = $p < 0.05$ as determined by a Student's *t* test.

stall the enzyme (22, 23, 42, 43). As seen in Fig. 1, this has significant biological ramifications for the expression of normally short-lived mRNAs in ZIKV-infected cells. Second, ZIKV and DENV-2 sfRNAs both interact with two other RNA decay factors, DDX6 and EDC3. Sequestration of these proteins could perhaps explain why sfRNA generation in flavivirus-infected cells influences not just 5′–3′-exonuclease activity, but also reduces decapping and deadenylation of transcripts (22, 23). Interestingly, a recently published sfRNA pulldown dataset indicates additional RNA decay factors may also interact with sfRNAs, including the deadenylase component CNOT1 (44). Third, sfRNAs interact with a variety of RNA-binding proteins that influence other post-transcriptional processes in the cell, including splicing and translation (Fig. 3). Knockdown and overexpression studies reported here on four of these sfRNA-interacting factors demonstrate that they have significant impact on the outcome of infection. Therefore, we conclude that the generation of sfRNA has broad implications for the RNA biology of the infected cell and illustrates the depth in which flaviviruses can dysregulate this important aspect of gene expression (Fig. 8).

XRN1 stalling and repression through the generation of sfRNAs appears to be a key characteristic common among members of the Flaviviridae that has evolved as a part of the molecular arms race to help the infecting virus usurp the innate immune response of the host. Notably, the strategy of targeting XRN1 is not unique to flaviviruses, but rather it appears to have evolved independently by other families of mammalian viruses as well. Indeed, recent studies from our lab and others demonstrate that the 3′ UTRs of several phleboviruses and arenaviruses contain RNA regions that effectively stall and repress XRN1 (43). Additionally, at least two segmented RNA plant viruses, red clover necrotic mosaic virus of the dianthoviruses of the Tombusviridae and beet necrotic yellow vein virus of the Benyviridae, also produce RNAs with the capability of stalling XRN1 (24, 42, 45, 46). Thus, XRN1 targeting appears to be a general strategy employed by RNA viruses from diverse evolutionary backgrounds to interface with the cytoplasmic RNA decay machinery.

There are a variety of reasons why RNA viruses might want to target the cytoplasmic 5′–3′-exoribonuclease XRN1. For one, XRN1 plays a major role in a key pathway of RNA decay that is responsible for regulating 20–50% of gene expression (47–49). Thus, the stalling and repression of this enzyme can significantly alter the regulation of host cell gene expression, as well as potentially limit the cell's ability to mount an active response to the virus infection. Additionally, there are reports suggesting that XRN1 is responsible for mediating the apparent cross-talk that occurs between the transcriptional machinery and the RNA decay machinery of the cell to maintain appropriate cel-

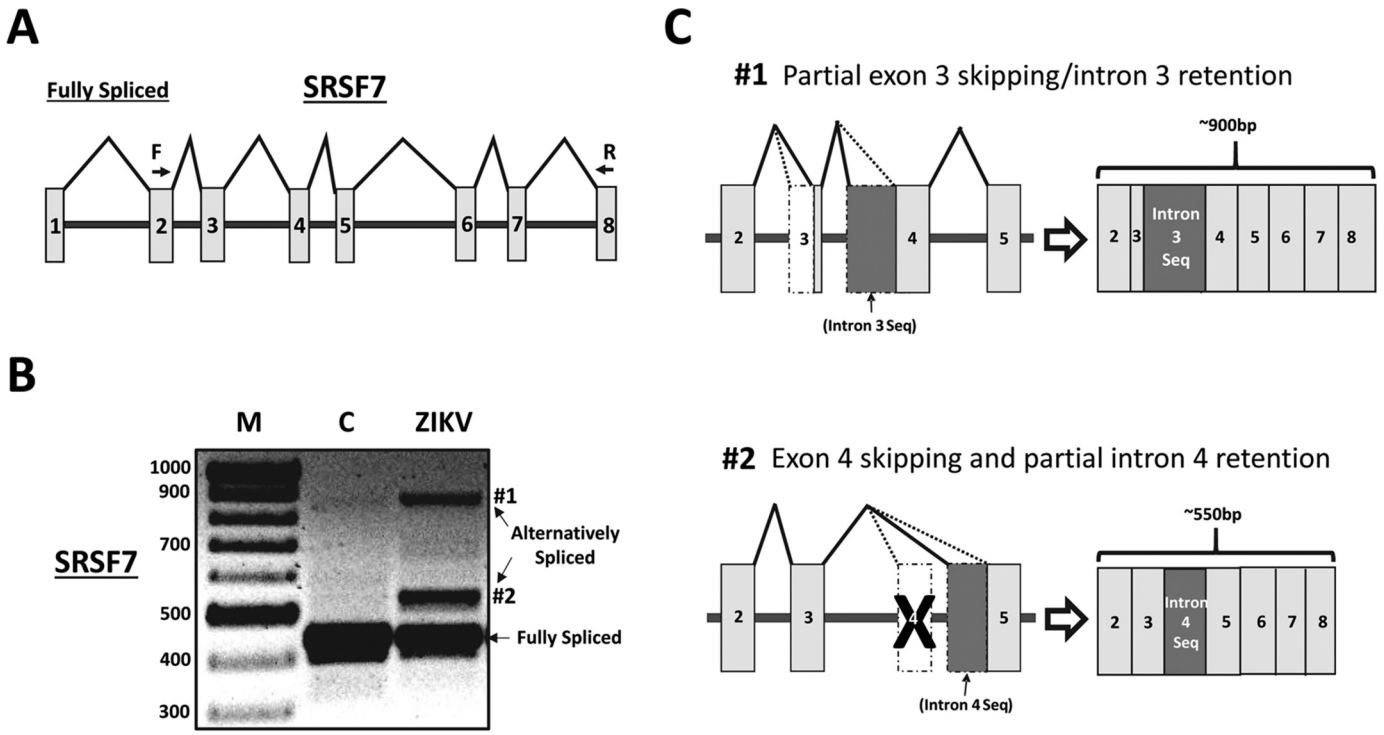

Figure 6. Splicing of *SF3B1* target gene is dysregulated during ZIKV infection. *A,* diagrammatic representation of the *SRSF7* gene exon–intron organization between exons 1 and 8. The relative position of PCR primers (forward (*F*) and reverse (*R*)) used to amplify the region of interest is also shown. *B,* total RNA from uninfected 293T cells (*lane C*) or 293T cells ZIKV infected at 48 hpi (*lane ZIKV*) was obtained and subjected to RT-PCR analysis using primers to amplify the region between exons 2 and 8. Products were electrophoresed on a 1% agarose gel and visualized by ethidium bromide staining. *C,* PCR products from *B* were gel-purified, cloned into a pGEM-T easy vector, and sequenced. The position of the resulting splice sites and exons for the indicated intermediates is indicated by the diagrams.

lular gene expression (50, 51). The act of targeting and repressing XRN1 by an RNA virus could therefore disrupt two distinct yet linked biological processes in the cell: RNA decay and transcription. Finally, XRN1 is a cytoplasmic enzyme readily accessible to RNA viruses that replicate in the cytoplasm. This arrangement greatly simplifies the dynamics of the viral infection as there is no need for the virus to transport targeting factors into the nucleus, which can require the assembly of specialized complexes (52).

Repression of cellular RNA decay, which results in the stabilization of normally short-lived cellular mRNAs (Fig. 1) (23), has broad implication for the cell. Short-lived mRNAs include many innate immune mediators and cytokines (53). Although overexpression of these immune factors seems at first to be counterproductive for a virus infection, overexpression can substantially dysregulate immune responses in the infected host as too much cytokine and chemokine production can inappropriately stimulate cells and wreak havoc for an effective immune response (54, 55). In addition, many cell cycle regulators and differentiation components are encoded by short-lived mRNAs (16). Repression of cellular RNA decay may therefore contribute in a significant fashion to the rewiring of cellular networks observed in flavivirus infections (56).

With roughly 94% of all human genes being alternatively spliced (57), it is perhaps not surprising that pathogens often target the splicing machinery to gain an upper hand during an infection (58). Transcriptome-wide analyses of ZIKV infections, for example, indicate that the virus affects RNA splicing in neural progenitor cells (4). Previous work has indicated that one way DENV-2 influences cellular RNA splicing is through the interaction of the viral NS5 protein with U5 snRNP core components CD2BP2 and DDX23 (59). The data presented here (Figs. 3 and 6) indicate that sfRNA sequestration of a number of splicing factors may also significantly contribute to the mis-regulation of cellular RNA splicing during infection. The PHAX and SF3B1 proteins found sequestered on both ZIKV and DENV sfRNAs are both attractive and available cellular protein targets for a cytoplasmic virus like Zika or dengue due to their dependence on nuclear/cytoplasmic shuttling (60, 61). Furthermore, SF3B1 has recently also been suggested to play a role in regulating transcription and chromatin modification (61, 62). SF3B1 inhibition results in complex splicing outcomes, including increased intron retention (63) and/or exon skipping (3). The results of our study indicate that both intron inclusion and exon skipping result from ZIKV infection, possibly due to SF3B1 sequestration on flaviviral sfRNAs (Fig. 6*C*).

The AID/APOBEC family of enzymes catalyze C-to-U deamination on single-stranded DNA or RNA. The APOBEC family members are evolutionarily conserved and share the structural and catalytic backbone of the zinc-dependent deaminase superfamily (9). APOBEC1 DNA-editing activity has also been shown to occur on herpes and hepatitis viral genomes (64, 65). Human APOBEC3G has a well-characterized defensive function in cells infected with HIV type 1 (HIV-1) (66). Interestingly APOBEC3G has been shown to be a cellular restriction factor against HCV replication (13). Instead of promoting editing of HCV RNAs, APOBEC3G appears to function instead by binding to the viral NS3 protein and decreasing its helicase

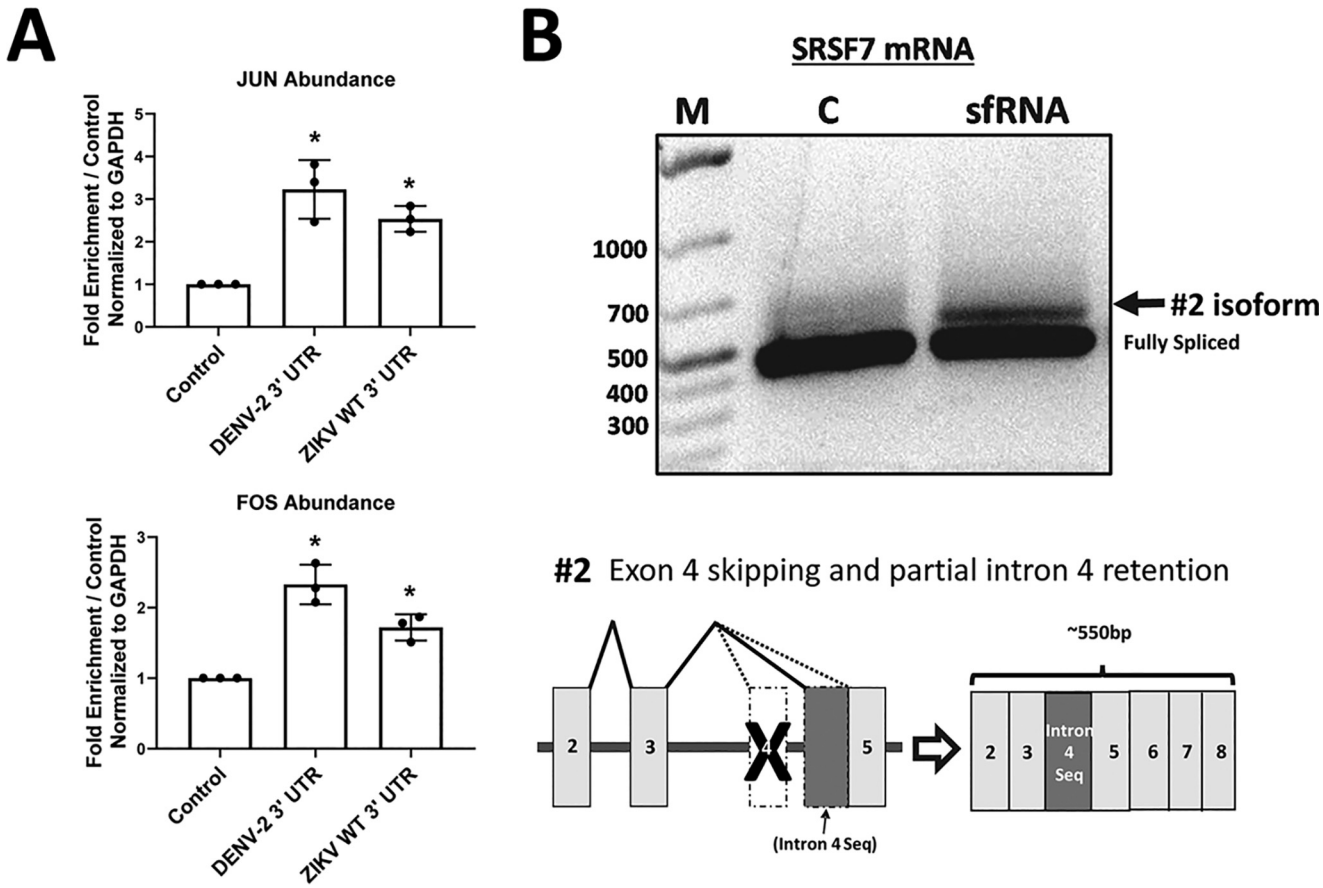

Figure 7. Transfection of sfRNA alone causes changes in cellular mRNA stability and splicing. *A,* HEK293T cells were transfected with RNAs containing the 3′ UTR of DENV-2, ZIKV, or a sized-matched unrelated control RNA. Total RNA was isolated 6 h post-transfection, and the abundance of the JUN and FOS mRNAs relative to the housekeeping GAPDH mRNA was assessed by quantitative RT-PCR. *B,* HEK293T cells were transfected with DENV-2 sfRNA or with a sized-matched unrelated control RNA (*C lane*). Total RNA was isolated 6 h post-transfection, and the splicing pattern of the *SRSF7* mRNAs was analyzed as described in Fig. 6. *M* refers to a lane with size markers. The position of the resulting splice sites and exons for the indicated *#2* splicing isoform is indicated by the diagram.

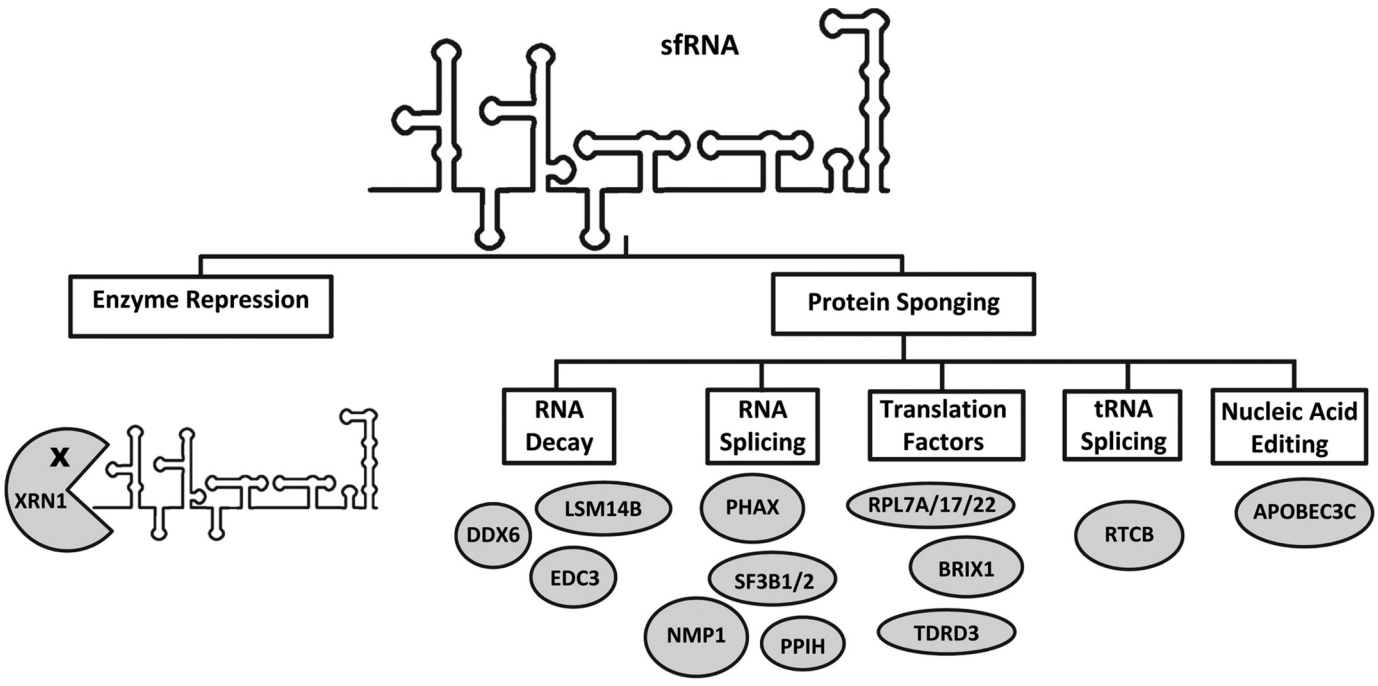

Figure 8. ZIKV and DENV sfRNAs bind a plethora of diverse RNA-binding proteins that can impact many post-transcriptional processes in the cell.

activity (14). Thus, because there is precedence in the literature for APOBEC-mediated restriction of RNA virus replication in a nonediting-based fashion, we hypothesize that the APOBEC3C enzyme is restricting ZIKV infection (Fig. 5) in a nonenzymatic way, perhaps through protein–protein and/or protein–RNA interactions.

In addition to the four factors pursued in this study, there were 15+ additional RNA-binding proteins identified with high confidence in our RNA pulldown/MS experiment that we have yet to explore in greater depth (Fig. 3*B*). This includes multiple host RNA-splicing factors in addition to PHAX and SF3B1 that could prove to play pivotal roles in mediating the significant degree of aberrant RNA splicing that is induced via flavivirus infection in human host cells. The interaction of sfRNA with translation factors (Fig. 3*B*) could of course play a significant role during infection in reprogramming protein synthesis to favor viral gene expression. Finally, RTCB, the catalytic component of the tRNA-splicing ligase complex, was also identified. RTCB also ligates RNA species besides spliced tRNAs, including fragments of the *XBP1* mRNA during endoplasmic reticulum stress/the unfolded protein response (67, 68). Given the impact of tRNA levels/codon optimality on gene expression (69) as well as the impact of the unfolded protein response on viral infections (70), it will be interesting to see if sfRNA-RTCB interactions are substantially impacting flavivirus infections.

Soto-Acosta *et al.* (77) recently reported the results of cellular proteins that associate with sfRNA from both the Asian and African lineages of ZIKV. Interestingly, they identified another RNA-binding protein that acts as a viral restriction factor (FMRP) and five other proteins, including the DDX6 protein discussed above. The differences in sfRNA protein association between this study and the one reported here likely reflect the stringency of the washing step in the pulldown, the differences in the set of RNAs used for the pulldown, and the exclusion parameters applied to determine hits. Nevertheless, the results of both studies lead to the conclusion that flavivirus sfRNAs are serving as biologically relevant sponges of cellular proteins during infection.

In closing, the detailed molecular mechanisms responsible for flavivirus-mediated cytopathology and pathogenesis remain relatively uncharacterized. Evidence is clearly accumulating that the noncoding sfRNA impacts virus–host interactions in a major fashion and thus is likely to impact disease processes. Therefore, minimizing the generation, accumulation, and/or function of sfRNAs could prove to be a viable target for therapeutics.

Experimental procedures

Northern blotting

For the detection of stable decay intermediates (sfRNAs) from ZIKV-infected cells, 1 μg of total cellular RNA was separated on a 5% polyacrylamide gel containing 7 M urea. The RNAs were transferred onto a nylon membrane (Hybond-XL; GE Healthcare) using a tank transfer unit. The blots were UV cross-linked and pre-washed with high stringency buffer (0.1× saline sodium citrate (SSC) buffer, 0.1% SDS) for 1 h at 60 °C with rotation. Blots were then prehybridized for 1 h at 60 °C in hybridization buffer (50% formamide, 1 mg/ml BSA, 750 mM NaCl, 75 mM sodium citrate, 0.1 mg/ml salmon sperm DNA, 1% SDS, 1 mg/ml polyvinylpyrrolidone, 1 mg/ml Ficoll). An *in vitro* transcribed, internally radiolabeled 428-base RNA probe complementary to the 3′ UTR of ZIKV (PRVABC59 strain) was gel-purified and incubated with the blot in hybridization buffer overnight at 60 °C. Blots were rinsed three times with low-stringency wash solution (2× SSC, 0.1% SDS) and three times with high-stringency wash solution (0.2× SSC, 0.1% SDS) for 15 min each at 60 °C. Hybridized RNAs were visualized by phosphorimaging on a Typhoon Trio Imager (GE Healthcare).

PCR and cloning

Cloning for XRN1 decay assays—The 3′ UTR sequences of ZIKV (PRVABC59-NCBI accession number KX377337) and DENV-2 (Jamaica/N.1409-NCBI accession number M20558) were used in this study. Four GeneArt String Fragments comprising the Zika virus 3′ UTR were obtained from Thermo Fisher Scientific as follows: WT ZIKV 3′ UTR (nucleotides 10,380 to 10,807); MUT1 (ZIKV 3′ UTR with a C→G transversion at position 10,416); MUT2- (ZIKV 3′ UTR with a C→G transversion at position 10,496); and DM- (ZIKV 3′ UTR with C→G transversions at positions 10,416 and 10.496). All viral 3′ UTR sequences were cloned into the polylinker region of the pGEM-4 vector (NCBI accession number X65303.1).

The reporter RNA (*CTRL lanes* in Fig. 2) for XRN1 biochemical assays was derived from pGem4 digested with EarI as described previously (22, 23). The nonspecific competitor RNA (control) was derived from pGem4 templates digested with SmlI. Preparation of the DENV-2 3′ UTR competitor RNA involved the PCR amplification of the proximal half of the DENV-2 3′ UTR (5′-AAGGCAAAACUAACAUGAAACAAGGCUAAAAGUCAGGUCGGAUCAAGCCAUAGUACGGAAAAAACUAUGCUACCUGUGAGCCCCGUCCAAGGACGUUAAAAGAAGUCAGGCCAUCACAAAUGCCACAGCUUGAGUAAACUGUGCAGCCUGUAGCUCCACCUGAGAAGGUGUAAAAAAUCUGGGAGGCCACAAACCAUGGAAGCUGUACGCAUGGCGUAG), which contains both XRN1 stalling three helix junction structures (18, 19). The amplified PCR product was cloned into pGem4 at the XbaI and HindIII sites, and the plasmid DNA was linearized with EarI.

Cloning for FLAG-tagged protein overexpression—cDNA from HEK293T cells was used as template for the PCR-based amplification of select open reading frames using sequence-specific primers engineered with restriction sites at their 5′ ends to allow for ligation into the polylinker region of p3XFLAG-CMV™-10 (Sigma). The primers used for this study were DDX6 NotI forward (5′-GATCGCGGCCGCGGAGCACGGCCAGAACAGAGAACC) and DDX6 BamHI reverse (5′-TCGCGGATCCTTAAGGTTTCTCATCTTCTACAGG); EDC3 EcoRI forward (5′-GATCGAATTCAGCTACAGATTGGCTGGGAAGTATTG) and EDC3 BamHI reverse (5′-TCGCGGATCCCTAAGCAGAGTGCAGTGGGATAAC); APOBEC3C EcoRI forward (5′-GATCGAATTCAAATCCACAGATCAGAAACCC) and APOBEC3C BamHI reverse (5′-TCGCGGATCCTCACTGGAGACTCTCCCGTA); and PHAX EcoRI- forward (5′-GATCGAATTCAGCGTTGGAG-

GTCGGCGATATG) and PHAX BamHI reverse (5′-TCGCGGATCCTTAAAAGATCTCCAAATCAT).

Cloning for splicing assays—cDNA from mock-infected or ZIKV-infected (48 hpi) HEK293T cells was used as template for the PCR-based amplification of the human *SRSF7* gene region spanning exons 2–8 using the following primers: SRSF7 Exon 2 forward, 5′-GAACTATCGACAGGCATGCC, and Exon 8 reverse, 5′-CTTCTGCGAGGACTTCCTGAT. PCR products were separated via agarose gel electrophoresis, and PCR products of interest were excised from the gel, purified using the Wizard SV gel, and the PCR extraction kit (Promega), and sequenced via Sanger sequencing. Sequencing reads were aligned using Serial Cloner software (version 2.6.1).

Cell lines and virus propagation

Human embryonic kidney 293T (HEK293T) and African green monkey kidney (*Cercopithecus aethiops*) (Vero) cells were maintained in Dulbecco's modified Eagle's medium (Mediatech-Corning) supplemented with 10% newborn calf serum (Peak Serum), 1% streptomycin/penicillin (Thermo Fisher Scientific-Hyclone), 0.5% L-glutamine (Thermo Fisher Scientific–Hyclone) and incubated at 37 °C in the presence of 5% CO_2. Human choriocarcinoma (JAR) cells were maintain in RPMI 1640 medium, 1× with L-glutamine (Corning) supplemented with 10% newborn calf serum, 1% streptomycin/penicillin, and 0.5% L-glutamine and incubated at 37 °C in the presence of 5% CO_2.

4SU metabolic labeling and mRNA half-life analysis

Maintenance media were replaced with fresh media containing 400 mM uridine analog 4SU as a metabolic label. RNA was collected 65 min after 4SU addition and fractionated as described previously (71). Total RNA was isolated using TRIzol (Invitrogen) and treated with DNase I (Fermentas). Reverse transcription was done using 1 μg of total RNA with Improm-II Reverse Transcriptase (Promega) and random hexamer primers to generate cDNA. The abundance of *GAPDH, FOS,* and *JUN* mRNAs was determined by quantitative digital droplet PCR using a QX200 Droplet Digital PCR System and QX200 EvaGreen ddPCR Supermix (Bio-Rad) and the following primers: *GAPDH* forward 5′-TCTTTTGCGTCGCCAGCCGA and *GAPDH* reverse 5′-ACCAGGCGCCCAATACGACC; *FOS* forward 5′-GTGGGAATGAAGTTGGCACT and *FOS* reverse 5′-CTACCACTCACCCGCAGACT; *JUN* forward 5′-GCCAGGTCGGCAGTATAGTC and *JUN* reverse 5′-TCTGGACATCCCGAAACAC. The data were normalized to *GAPDH* across all samples and fold-changes in the target mRNA were calculated using QuantSoft software. The data shown represent the mean values from three independent experiments. *p* values were determined by a Student's *t* test using GraphPad Prism software.

RNA–protein reconstitution, purification, and MS

pGEM4, or derivatives harboring the ZIKV 3′ UTR, or DENV-2 3′ UTR sequences downstream of a SP6 promoter sequence were linearized via restriction enzyme digestion, and *in vitro* transcription reactions were performed in the presence of Biotin-14–CTP (Thermo Fisher Scientific) to generate biotinylated RNAs capable of downstream isolation via streptavidin magnetic beads. Newly transcribed RNAs were extracted using phenol/chloroform/isoamyl alcohol (24:25:1), ethanol-precipitated using 10 M ammonium acetate, and resuspended in double-distilled H_2O. Biotinylated RNAs were quantified using a Nanodrop 2000c (Thermo Fisher Scientific). 1 μg of each biotinylated RNA was incubated for 10 min at room temperature with 100 μl of uMacs streptavidin magnetic beads (Miltenyi Biotec). uMacs magnetic bead columns were equilibrated and rinsed two times with Binding buffer (10 mM HEPES, pH 7.0, 50 mM KCl, 10% glycerol, 1 mM EDTA, 1 mM DTT, 0.5% Triton X-100, and Ribolock RNase inhibitor) (Thermo Fisher Scientific). Pre-cleared HeLa cell cytoplasmic extract (prepared as described in refs. 72, 73) supplemented with 5 μl of protease inhibitor mixture (Sigma) was added to each reaction tube and incubated at 4 °C with rotation for 60 min. Columns were washed four times with 1 ml of Wash buffer (Binding buffer supplemented with 250 mM KCl). RNA-binding proteins (RBPs) were eluted from the RNAs via the addition of Binding buffer supplemented with 1 M NaCl. Equal volumes of eluted RBPs were electrophoresed into a 10% SDS-PAGE. Proteins were Coomassie-stained, excised from the gel, and submitted to the Proteomics and Metabolomics Facility at Colorado State University for trypsin digestion and LC-MS/MS protein identification.

Tandem mass spectra were extracted, charge state deconvoluted, and deisotoped by ProteoWizard MsConvert (version 3.0). Spectra from all samples were searched using Mascot (Matrix Science, London, UK; version 2.3.01) against the Uniprot_Human_rev_071916 database (185,161 entries) assuming the digestion enzyme trypsin. Mascot was searched with a fragment ion mass tolerance of 0.80 Da and a parent ion tolerance of 20 ppm. Oxidation of methionine, carbamidomethyl of cysteine, and carboxymethyl of cysteine were specified in Mascot as variable modifications. Search results from all samples were imported and combined using the probabilistic protein identification algorithms implemented in Scaffold software (version 4.5.1, Proteome Software Inc., Portland, OR). Peptide thresholds (95%) were set such that a peptide false discovery rate of 0.0% was achieved based on hits to the reverse database. Protein identifications were accepted if they could be established at greater than 95.0% probability and contained at least two identified peptides. Protein probabilities were assigned by the Protein Prophet algorithm. Proteins that contained similar peptides and could not be differentiated based on MS/MS analysis alone were grouped to satisfy the principles of parsimony. The number of missed and/or nonspecific cleavages permitted in the MS search parameters was three.

The MS proteomics data have been deposited to the ProteomeXchange Consortium via the PRIDE partner repository with the dataset identifier PXD014933 and 10.6019/PXD014933.

siRNA knockdown in ZIKV-infected HEK293T cells

HEK293T cells (~30% confluent) were transfected with either control siRNA or targeting siRNAs using jetPrime transfection reagent (Polyplus) according to the manufacturer's instructions. The transfection was repeated 24 h later to ensure

efficient knockdown. The next day, cells were infected with ZIKV (m.o.i. = 10) and transfected 1 h later with another round of siRNAs. After 48 h, media were harvested for the analysis of infectious virus, and total RNA/protein was generated using TRIzol and treated with DNase I. Reverse transcription was done using 1 μg of total RNA with Improm-II reverse transcriptase and random hexamer primers to generate cDNA. The abundance levels of *GAPDH* mRNA, mRNAs targeted via the siRNAs for knockdown, and ZIKV RNA were determined by quantitative digital droplet PCR using the Bio-Rad QX200 Droplet Digital PCR System and QX200 EvaGreen ddPCR Supermix as outlined above. The primers used were as follows: *GAPDH* forward 5′-TCTTTTGCGTCGCCAGCCGA and *GAPDH* reverse 5′-ACCAGGCGCCCAATACGACC; and *ZIKV* RNA forward 5′-AGGATCATAGGTGATGAAGAAAAGT and *ZIKV* RNA reverse 5′-GCACCAATCTTAATGTTGTCAGG. The data shown represent the mean values from three independent experiments. *p* values were determined by a Student's *t* test using GraphPad Prism software.

Protein pellets from TRIzol samples were resuspended in a 3:1 mixture of 8 M urea, 1% SDS and concentrations determined using a Qubit 3.0 fluorometer and Qubit Protein Assay kit (Thermo Fisher Scientific). Equal weight of protein from each sample was then separated via SDS-PAGE. Proteins were transferred to polyvinylidene difluoride membranes (Immobilon-P) using a semi-dry electrophoretic transfer cell (Bio-Rad). Transferred blots were blocked in blocking buffer (1× PBS/Tween 20 supplemented with 5% powdered milk) for 60 min at room temperature with rotation. Blots were probed by rotating the blot in the presence of primary antibodies in fresh blocking buffer. Blots were washed three times with 1× PBS/Tween 20 and incubated with secondary antibody in fresh blocking buffer for 60 min at room temperature. Blots were washed three times with 1× PBS/Tween 20 solution and developed using SuperSignal West Dura extended duration substrate (Thermo Fisher Scientific). Blots were imaged using the Azure Sapphire Biomolecular Imager. Antibodies used in this study were APOBEC3C (GeneTex GTX102164), PHAX (Abcam ab157096), SF3B1 (Abcam ab667774), GAPDH (Millipore Sigma clone 6C5), FLAG (Millipore Sigma F1804-200UG), anti-mouse secondary (Santa Cruz Biotechnology sc-2005) and anti-rabbit secondary (Santa Cruz Biotechnology sc-2030).

Protein overexpression in ZIKV-infected HEK293T cells

HEK293T cells (~30% confluent) were transfected with p3XFLAG-CMV^{TM}-10 harboring the protein of interest or no inserted sequence (empty vector) using jetPrime transfection reagent. The transfection was repeated 24 h later to optimize efficient protein expression. The next day, cells were infected with ZIKV (m.o.i. = 10) and transfected 1 h later with another round of expression vector. After 48 h, media were harvested for the analysis of infectious virus and total RNA/protein as described above.

Virus preparation

Infectious Zika virus (strain PRVABC59) was generated from infectious cDNA clones (74). Virus was propagated in Vero cells and titered via focus-forming assays as described previously (75).

XRN1 biochemical assays

RNAs were *in vitro* transcribed using SP6 polymerase in the presence of a 10× molar excess of 5′-GMP to GTP in the reaction to obtain transcripts with a 5′-monophosphate (22, 23). Approximately 30 femtomoles of radioactive RNAs was incubated with either recombinant yeast XRN1 protein (New England Biolabs), HeLa cytoplasmic extracts, or C6/36 cytoplasmic S100 extracts prepared as described previously (72–73) under conditions that promote 5′–3′-exonucleolytic decay (76). Reaction products were analyzed on 5% polyacrylamide gels containing 7 M urea and visualized by phosphorimaging.

In vivo formaldehyde cross-linking and RNA co-immunoprecipitation analysis

ZIKV-infected HEK293T cells were collected at 48 hpi, washed, and resuspended in 10 ml of 1× PBS. Formaldehyde was added to the tubes to a final concentration of 0.3% and incubated at room temperature for 10 min. 2 M glycine, pH 7.0, was added; cells were washed with PBS, and whole-cell lysates were generated by resuspending the cells in low-stringency RIPA buffer (50 mM Tris-HCl, pH 7.5, 1% Nonidet P-40, 0.5% sodium deoxycholate, 0.05% SDS, 1 mM EDTA, 150 mM NaCl) supplemented with 0.2 mM PMSF and protease inhibitor mixture (Sigma). The lysate was filtered through a 26-gauge needle, centrifuged to pellet debris, and pre-cleared by incubating with protein A magnetic beads (New England Biolabs). Beads were separated from cleared supernatant, and a portion of the lysate was set aside as "Input." The remaining lysate was divided into two equal portions and diluted with low-stringency RIPA buffer. Primary antibody or normal rabbit IgG was added, and the reaction was incubated for 1 h at 4 °C. Protein A magnetic beads were added, and the mixtures were incubated at 4 °C for an additional hour. The beads were then washed five times with high-stringency RIPA buffer (50 mM Tris-HCl, pH 7.5, 1% Nonidet P-40, 1% sodium deoxycholate, 0.1% SDS, 1 mM EDTA, 1 M NaCl, 1 M urea) supplemented with 1 mM PMSF and protease inhibitor mixture. Beads were resuspended in TEDS buffer (50 mM Tris-HCl, pH 7.0, 5 mM EDTA, 10 mM dithiothreitol (DTT), and 1% SDS) and incubated at 70 °C for 45 min to reverse cross-linking. TRIzol was added to each reaction, and RNA was isolated following the manufacturer's protocol. Reverse transcription was performed using 1 μg of total RNA and analyzed by ddPCR as described above.

RNA transfections

RNAs containing the entire DENV-2 3′ UTR, ZIKV 3′ UTR, or a size-matched control transcript derived from the pGEM4 plasmid cut with SmlI were transcribed using the MEGAscript SP6 kit (Thermo Fisher Scientific) supplementing the reactions with 100 mM GMP to generate GMP 5′-end-labeled transcripts and purified. HEK293T cells were transfected using Lipofectamine 2000 and 5 μg of RNA. Total cellular RNA was isolated using TRIzol at 6 h post-transfection and samples were analyzed as described above.

Library preparation and RNA-Seq

Sequencing libraries were prepared from 4SU-labeled, ZIKV-infected JAR cells at 12 and 72 hpi (see under "4SU metabolic labeling and mRNA half-life analysis" and under "siRNA knockdown in ZIKV-infected HEK293T cells" and "Protein overexpression in ZIKV-infected HEK293T cells" above). Libraries were constructed from 500 ng of total RNA. First-strand cDNA synthesis and PCR amplification were performed using the SMARTe^{TM} PCR cDNA synthesis kit and Advantage 2 PCR kit (Clontech) in accordance with manufacturer's protocols. Amplified libraries were tagmented using a Tn5 tagmentation enzyme generously provided by Dr. Mark Stenglein. Preparation of the enzyme and reactions conditions were performed in accordance with a previously published protocol (78). Following tagmentation, libraries were evaluated for a median product size of 200–300 bp using the Agilent TapeStation 2200, D1000 ScreenTape, and reagents. Concentrations were measured fluorometrically via Qubit (Thermo Fisher Scientific), and equal masses, 10 ng, of each sample were pooled together. Final library quantification was performed by the Colorado State University NGS Core using the Illumina library quantification kit (KAPA Biosystems) per the manufacturer's protocols. Sequencing was performed on an Illumina NextSeq 500 instrument using single-end 1 × 75 sequencing from a NextSeq 500/550 high output kit version 2 (75 cycles) (Illumina). The mean number of reads per sample was 20–30 million.

SLAM-DUNK analysis

FastQC version 0.11.5 was utilized to assess the quality of sequence reads. Reads were trimmed of adapter sequences and filtered for low-complexity or low-quality reads using Trimmomatic version 0.32. rRNA reads were filtered out using Bowtie2 version 2.3.4.3 and a reference fasta file of mature 5S, 18S, and 28S rRNA sequences obtained from NCBI RefSeq. The SLAMDUNK package (79) was used to map reads to the hg19 genome, call single-nucleotide polymorphisms, and count relevant statistics for the 3′ UTRs of genes. Base conversion ratios for each sample were calculated using the alleyoop rates command. Mean base conversion ratios were calculated for 12 and 72 hpi and reported.

Raw and processed RNA-seq data generated in this study, as well as the 3′ UTR reference and rRNA fasta files used, were uploaded to the NCBI Gene Expression Omnibus (GEO) database under the accession number GSE135413.

Author contributions—D. M., J. G. O., J. R., P. A. C., and B. J. G. investigation; D. M., J. R., and J. R. A. methodology; D. M., J. G. O., and J. W. writing-original draft; D. M., J. R., P. A. C., J. R. A., A. M. H., B. J. G., and J. W. writing-review and editing; J. R. and J. W. conceptualization; A. M. H. data curation; A. M. H. formal analysis; B. J. G. and J. W. funding acquisition; B. J. G. and J. W. project administration.

Acknowledgments—We thank Carol Wilusz and members of the Wilusz and Geiss labs for helpful discussions.

References

1. Cross, S. T., Michalski, D., Miller, M. R., and Wilusz, J. (2019) RNA regulatory processes in RNA virus biology. *Wiley Interdiscip. Rev. RNA* **10,** e1536 CrossRef Medline
2. Darman, R. B., Seiler, M., Agrawal, A. A., Lim, K. H., Peng, S., Aird, D., Bailey, S. L., Bhavsar, E. B., Chan, B., Colla, S., Corson, L., Feala, J., Fekkes, P., Ichikawa, K., Keaney, G. F., *et al.* (2015) Cancer-associated SF3B1 hotspot mutations induce cryptic 3′ splice site selection through use of a different branch point. *Cell Rep.* **13,** 1033–1045 CrossRef Medline
3. Wu, G., Fan, L., Edmonson, M. N., Shaw, T., Boggs, K., Easton, J., Rusch, M. C., Webb, T. R., Zhang, J., and Potter, P. M. (2018) Inhibition of SF3B1 by molecules targeting the spliceosome results in massive aberrant exon skipping. *RNA* **24,** 1056–1066 CrossRef Medline
4. Hu, B., Huo, Y., Yang, L., Chen, G., Luo, M., Yang, J., and Zhou, J. (2017) ZIKV infection effects changes in gene splicing, isoform composition and lncRNA expression in human neural progenitor cells. *Virol. J.* **14,** 217 CrossRef Medline
5. Schoenberg, D. R., and Maquat, L. E. (2012) Regulation of cytoplasmic mRNA decay. *Nat. Rev. Genet.* **13,** 246–259 CrossRef Medline
6. Moon, S. L., and Wilusz, J. (2013) Cytoplasmic viruses: rage against the (cellular RNA decay) machine. *PLoS Pathog.* **9,** e1003762 CrossRef Medline
7. Schott, J., and Stoecklin, G. (2010) Networks controlling mRNA decay in the immune system. *Wiley Interdiscip. Rev. RNA* **1,** 432–456 CrossRef Medline
8. Kung, C., Maggi, L. B., and Weber, J. D. (2018) The role of RNA editing in cancer development and metabolic disorders. *Front. Endocrinol.* (*Lausanne*) **9,** 762 CrossRef Medline
9. Lerner, T., Papavasiliou, F. N., and Pecori, R. (2018) RNA editors, cofactors, and mRNA targets: an overview of the C-to-U RNA editing machinery and its implication in human disease. *Genes* (*Basel*) **10,** 13 CrossRef Medline
10. Sharma, S., Patnaik, S. K., Taggart, R. T., Kannisto, E. D., Enriquez, S. M., Gollnick, P., and Baysal, B. E. (2015) APOBEC3A cytidine deaminase induces RNA editing in monocytes and macrophages. *Nat. Commun.* **6,** 6881 CrossRef Medline
11. Sharma, S., Patnaik, S. K., Taggart, R. T., and Baysal, B. E. (2016) The double-domain cytidine deaminase APOBEC3G is a cellular site-specific RNA editing enzyme. *Sci. Rep.* **6,** 39100 CrossRef Medline
12. Chemudupati, M., Kenney, A. D., Bonifati, S., Zani, A., McMichael, T. M., Wu, L., and Yount, J. S. (2019) From APOBEC to ZAP: diverse mechanisms used by cellular restriction factors to inhibit virus infections. *Biochim. Biophys. Acta* **1866,** 382–394 CrossRef Medline
13. Peng, Z.-G., Zhao, Z.-Y., Li, Y.-P., Wang, Y.-P., Hao, L.-H., Fan, B., Li, Y.-H., Wang, Y.-M., Shan, Y.-Q., Han, Y.-X., Zhu, Y. P., Li, J. R., You, X. F., Li, Z. R., and Jiang, J. D. (2011) Host apolipoprotein B messenger RNA-editing enzyme catalytic polypeptide-like 3G is an innate defensive factor and drug target against hepatitis C virus. *Hepatology* **53,** 1080–1089 CrossRef Medline
14. Zhu, Y.-P., Peng, Z.-G., Wu, Z.-Y., Li, J.-R., Huang, M.-H., Si, S.-Y., and Jiang, J.-D. (2015) Host APOBEC3G protein inhibits HCV replication through direct binding at NS3. *PLoS ONE* **10,** e0121608 CrossRef Medline
15. Ferguson, N. M. (2018) Challenges and opportunities in controlling mosquito-borne infections. *Nature* **559,** 490–497 CrossRef Medline
16. Slonchak, A., and Khromykh, A. A. (2018) Subgenomic flaviviral RNAs: what do we know after the first decade of research. *Antiviral. Res.* **159,** 13–25 CrossRef Medline
17. Pijlman, G. P., Funk, A., Kondratieva, N., Leung, J., Torres, S., van der Aa L., Liu, W. J., Palmenberg, A. C., Shi, P.-Y., Hall, R. A., and Khromykh, A. A. (2008) A highly structured, nuclease-resistant, noncoding RNA produced by flaviviruses is required for pathogenicity. *Cell Host Microbe* **4,** 579–591 CrossRef Medline
18. Funk, A., Truong, K., Nagasaki, T., Torres, S., Floden, N., Balmori Melian, E., Edmonds, J., Dong, H., Shi, P.-Y., and Khromykh, A. A. (2010) RNA structures required for production of subgenomic flavivirus RNA. *J. Virol.* **84,** 11407–11417 CrossRef Medline

19. Silva, P. A., Pereira, C. F., Dalebout, T. J., Spaan, W. J., and Bredenbeek, P. J. (2010) An RNA pseudoknot is required for production of yellow fever virus subgenomic RNA by the host nuclease XRN1. *J. Virol.* **84,** 11395–11406 CrossRef Medline
20. Chapman, E. G., Moon, S. L., Wilusz, J., and Kieft, J. S. (2014) RNA structures that resist degradation by Xrn1 produce a pathogenic Dengue virus RNA. *Elife* **3,** e01892 CrossRef Medline
21. Chapman, E. G., Costantino, D. A., Rabe, J. L., Moon, S. L., Wilusz, J., Nix, J. C., and Kieft, J. S. (2014) The structural basis of pathogenic subgenomic flavivirus RNA (sfRNA) production. *Science* **344,** 307–310 CrossRef Medline
22. Moon, S. L., Anderson, J. R., Kumagai, Y., Wilusz, C. J., Akira, S., Khromykh, A. A., and Wilusz, J. (2012) A noncoding RNA produced by arthropod-borne flaviviruses inhibits the cellular exoribonuclease XRN1 and alters host mRNA stability. *RNA* **18,** 2029–2040 CrossRef Medline
23. Moon, S. L., Blackinton, J. G., Anderson, J. R., Dozier, M. K., Dodd, B. J., Keene, J. D., Wilusz, C. J., Bradrick, S. S., and Wilusz, J. (2015) XRN1 stalling in the 5′ UTR of hepatitis C virus and bovine viral diarrhea virus is associated with dysregulated host mRNA stability. *PLoS Pathog.* **11,** e1004708 CrossRef Medline
24. Steckelberg, A.-L., Akiyama, B. M., Costantino, D. A., Sit, T. L., Nix, J. C., and Kieft, J. S. (2018) A folded viral noncoding RNA blocks host cell exoribonucleases through a conformationally dynamic RNA structure. *Proc. Natl. Acad. Sci. U.S.A.* **115,** 6404–6409 CrossRef Medline
25. Yeh, S.-C., and Pompon, J. (2018) Flaviviruses produce a subgenomic flaviviral RNA that enhances mosquito transmission. *DNA Cell Biol.* **37,** 154–159 CrossRef Medline
26. Pompon, J., Manuel, M., Ng, G. K., Wong, B., Shan, C., Manokaran, G., Soto-Acosta, R., Bradrick, S. S., Ooi, E. E., Missé, D., Shi, P. Y., and Garcia-Blanco, M. A. (2017) Dengue subgenomic flaviviral RNA disrupts immunity in mosquito salivary glands to increase virus transmission. *PLoS Pathog.* **13**, e1006535 CrossRef Medline
27. Göertz, G. P., Fros, J. J., Miesen, P., Vogels, C. B. F., van der Bent, M. L., Geertsema, C., Koenraadt, C. J. M., van Rij, R. P., van Oers, M. M., and Pijlman, G. P. (2016) Noncoding subgenomic flavivirus RNA is processed by the mosquito RNA interference machinery and determines West Nile virus transmission by Culex pipiens mosquitoes. *J. Virol.* **90,** 10145–10159 CrossRef Medline
28. Manokaran, G., Finol, E., Wang, C., Gunaratne, J., Bahl, J., Ong, E. Z., Tan, H. C., Sessions, O. M., Ward, A. M., Gubler, D. J., Harris, E., Garcia-Blanco, M. A., and Ooi, E. E. (2015) Dengue subgenomic RNA binds TRIM25 to inhibit interferon expression for epidemiological fitness. *Science* **350,** 217–221 CrossRef Medline
29. Bidet, K., and Garcia-Blanco, M. A. (2014) Flaviviral RNAs: weapons and targets in the war between virus and host. *Biochem. J.* **462,** 215–230 CrossRef Medline
30. Schnettler, E., Sterken, M. G., Leung, J. Y., Metz, S. W., Geertsema, C., Goldbach, R. W., Vlak, J. M., Kohl, A., Khromykh, A. A., and Pijlman, G. P. (2012) Noncoding flavivirus RNA displays RNA interference suppressor activity in insect and mammalian cells. *J. Virol.* **86,** 13486–13500 CrossRef Medline
31. Schuessler, A., Funk, A., Lazear, H. M., Cooper, D. A., Torres, S., Daffis, S., Jha, B. K., Kumagai, Y., Takeuchi, O., Hertzog, P., Silverman, R., Akira, S., Barton, D. J., Diamond, M. S., and Khromykh, A. A. (2012) West Nile virus noncoding subgenomic RNA contributes to viral evasion of the type I interferon-mediated antiviral response. *J. Virol.* **86,** 5708–5718 CrossRef Medline
32. Moon, S. L., Dodd, B. J., Brackney, D. E., Wilusz, C. J., Ebel, G. D., and Wilusz, J. (2015) Flavivirus sfRNA suppresses antiviral RNA interference in cultured cells and mosquitoes and directly interacts with the RNAi machinery. *Virology* **485,** 322–329 CrossRef Medline
33. Gutiérrez-Bugallo, G., Piedra, L. A., Rodriguez, M., Bisset, J. A., Lourenço-de-Oliveira, R., Weaver, S. C., Vasilakis, N., and Vega-Rúa, A. (2019) Vector-borne transmission and evolution of Zika virus. *Nat. Ecol. Evol.* **3,** 561–569 CrossRef Medline
34. Pierson, T. C., and Diamond, M. S. (2018) The emergence of Zika virus and its new clinical syndromes. *Nature* **560,** 573–581 CrossRef Medline
35. Miner, J. J., and Diamond, M. S. (2017) Zika virus pathogenesis and tissue tropism. *Cell Host Microbe* **21,** 134–142 CrossRef Medline
36. Akiyama, B. M., Laurence, H. M., Massey, A. R., (2016) Zika virus produces noncoding RNAs using a multipseudoknot structure that confounds a cellular exonuclease. *Science* **354,** 1148–1152 CrossRef Medline
37. Ostareck, D. H., Naarmann-de Vries, I. S., and Ostareck-Lederer, A. (2014) DDX6 and its orthologs as modulators of cellular and viral RNA expression. *Wiley Interdiscip. Rev. RNA* **5,** 659–678 CrossRef Medline
38. Scheller, U., Pfisterer, K., Uebe, S., Ekici, A. B., Reis, A., Jamra, R., and Ferrazzi, F. (2018) Integrative bioinformatics analysis characterizing the role of EDC3 in mRNA decay and its association to intellectual disability. *BMC Med. Genomics* **11,** 41 CrossRef Medline
39. Boulon, S., Verheggen, C., Jady, B. E., Girard, C., Pescia, C., Paul, C., Ospina, J. K., Kiss, T., Matera, A. G., Bordonné, R., and Bertrand, E. (2004) PHAX and CRM1 are required sequentially to transport U3 snoRNA to nucleoli. *Mol. Cell* **16,** 777–787 CrossRef Medline
40. Siriwardena, S. U., Chen, K., and Bhagwat, A. S. (2016) Functions and malfunctions of mammalian DNA-cytosine deaminases. *Chem. Rev.* **116,** 12688–12710 CrossRef Medline
41. Smith, H. C. (2017) RNA binding to APOBEC deaminases; not simply a substrate for C to U editing. *RNA Biol.* **14,** 1153–1165 CrossRef Medline
42. Flobinus, A., Chevigny, N., Charley, P. A., Seissler, T., Klein, E., Bleykasten-Grosshans, C., Ratti, C., Bouzoubaa, S., Wilusz, J., and Gilmer, D. (2018) Beet necrotic yellow vein virus noncoding RNA production depends on a 5′→3′ Xrn exoribonuclease activity. *Viruses* **10,** 137 CrossRef Medline
43. Charley, P. A., Wilusz, C. J., and Wilusz, J. (2018) Identification of phlebovirus and arenavirus RNA sequences that stall and repress the exoribonuclease XRN1. *J. Biol. Chem.* **293,** 285–295 CrossRef Medline
44. Liao, K.-C., Chuo, V., Ng, W. C., Neo, S. P., Pompon, J., Gunaratne, J., Ooi, E. E., and Garcia-Blanco, M. A. (2018) Identification and characterization of host proteins bound to dengue virus 3′ UTR reveal an antiviral role for quaking proteins. *RNA* **24,** 803–814 CrossRef Medline
45. Iwakawa, H.-O., Mizumoto, H., Nagano, H., Imoto, Y., Takigawa, K., Sarawaneeyaruk, S., Kaido, M., Mise, K., and Okuno, T. (2008) A viral noncoding RNA generated by cis-element-mediated protection against 5′ → 3′. RNA decay represses both cap-independent and cap-dependent translation. *J. Virol.* **82,** 10162–10174 CrossRef Medline
46. Flobinus, A., Hleibieh, K., Klein, E., Ratti, C., Bouzoubaa, S., and Gilmer, D. (2016) A viral noncoding RNA complements a weakened viral RNA silencing suppressor and promotes efficient systemic host infection. *Viruses* **8,** 272 CrossRef Medline
47. Cheadle, C., Fan, J., Cho-Chung, Y. S., Werner, T., Ray, J., Do, L., Gorospe, M., and Becker, K. G. (2005) Stability regulation of mRNA and the control of gene expression. *Ann. N.Y. Acad. Sci.* **1058,** 196–204 CrossRef Medline
48. García-Martínez, J., Aranda, A., and Pérez-Ortín, J. E. (2004) Genomic run-on evaluates transcription rates for all yeast genes and identifies gene regulatory mechanisms. *Mol. Cell* **15,** 303–313 CrossRef Medline
49. Schwanhäusser, B., Busse, D., Li, N., Dittmar, G., Schuchhardt, J., Wolf, J., Chen, W., and Selbach, M. (2011) Global quantification of mammalian gene expression control. *Nature* **473,** 337–342 CrossRef Medline
50. Haimovich, G., Medina, D. A., Causse, S. Z., Garber, M., Millán-Zambrano, G., Barkai, O., Chávez, S., Pérez-Ortín, J. E., Darzacq, X., and Choder, M. (2013) Gene expression is circular: factors for mRNA degradation also foster mRNA synthesis. *Cell* **153,** 1000–1011 CrossRef Medline
51. Sun, M., Schwalb, B., Pirkl, N., Maier, K. C., Schenk, A., Failmezger, H., Tresch, A., and Cramer, P. (2013) Global analysis of eukaryotic mRNA degradation reveals Xrn1-dependent buffering of transcript levels. *Mol. Cell* **52,** 52–62 CrossRef Medline
52. Raices, M., and D'Angelo, M. A. (2017) Nuclear pore complexes and regulation of gene expression. *Curr. Opin. Cell Biol.* **46,** 26–32 CrossRef Medline
53. Ezegbunam, W., and Foronjy, R. (2018) Post-transcriptional control of airway inflammation. *Wiley Interdiscip. Rev. RNA* **9,** e1455 CrossRef Medline
54. Suthar, M. S., Diamond, M. S., and Gale, M. (2013) West Nile virus infection and immunity. *Nat. Rev. Microbiol.* **11,** 115–128 CrossRef Medline

55. St John, A. L., Abraham, S. N., and Gubler, D. J. (2013) Barriers to preclinical investigations of anti-dengue immunity and dengue pathogenesis. *Nat. Rev. Microbiol.* **11,** 420–426 CrossRef Medline
56. Neufeldt, C. J., Cortese, M., Acosta, E. G., and Bartenschlager, R. (2018) Rewiring cellular networks by members of the Flaviviridae family. *Nat. Rev. Microbiol.* **16,** 125–142 CrossRef Medline
57. Wang, E. T., Sandberg, R., Luo, S., Khrebtukova, I., Zhang, L., Mayr, C., Kingsmore, S. F., Schroth, G. P., and Burge, C. B. (2008) Alternative isoform regulation in human tissue transcriptomes. *Nature* **456,** 470–476 CrossRef Medline
58. Ashraf, U., Benoit-Pilven, C., Lacroix, V., Navratil, V., and Naffakh, N. (2019) Advances in analyzing virus-induced alterations of host cell splicing. *Trends Microbiol.* **27,** 268–281 CrossRef Medline
59. De Maio, F. A., Risso, G., Iglesias, N. G., Shah, P., Pozzi, B., Gebhard, L. G., Mammi, P., Mancini, E., Yanovsky, M. J., Andino, R., Krogan, N., Srebrow, A., and Gamarnik, A. V. (2016) The dengue virus NS5 protein intrudes in the cellular spliceosome and modulates splicing. *PLoS Pathog.* **12,** e1005841 CrossRef Medline
60. Mourão, A., Varrot, A., Mackereth, C. D., Cusack, S., and Sattler, M. (2010) Structure and RNA recognition by the snRNA and snoRNA transport factor PHAX. *RNA* **16,** 1205–1216 CrossRef Medline
61. Kfir, N., Lev-Maor, G., Glaich, O., Alajem, A., Datta, A., Sze, S. K., Meshorer, E., and Ast, G. (2015) SF3B1 association with chromatin determines splicing outcomes. *Cell Rep.* **11,** 618–629 CrossRef Medline
62. Girard, C., Will, C. L., Peng, J., Makarov, E. M., Kastner, B., Lemm, I., Urlaub, H., Hartmuth, K., and Lührmann, R. (2012) Post-transcriptional spliceosomes are retained in nuclear speckles until splicing completion. *Nat. Commun.* **3,** 994 CrossRef Medline
63. Yoshimoto, R., Kaida, D., Furuno, M., Burroughs, A. M., Noma, S., Suzuki, H., Kawamura, Y., Hayashizaki, Y., Mayeda, A., and Yoshida, M. (2017) Global analysis of pre-mRNA subcellular localization following splicing inhibition by spliceostatin A. *RNA* **23,** 47–57 CrossRef Medline
64. Gee, P., Ando, Y., Kitayama, H., Yamamoto, S. P., Kanemura, Y., Ebina, H., Kawaguchi, Y., and Koyanagi, Y. (2011) APOBEC1-mediated editing and attenuation of herpes simplex virus 1 DNA indicate that neurons have an antiviral role during herpes simplex encephalitis. *J. Virol.* **85,** 9726–9736 CrossRef Medline
65. Gonzalez, M. C., Suspène, R., Henry, M., Guétard, D., Wain-Hobson, S., and Vartanian, J. P. (2009) Human APOBEC1 cytidine deaminase edits HBV DNA. *Retrovirology* **6,** 96 CrossRef Medline
66. Sheehy, A. M., Gaddis, N. C., Choi, J. D., and Malim, M. H. (2002) Isolation of a human gene that inhibits HIV-1 infection and is suppressed by the viral Vif protein. *Nature* **418,** 646–650 CrossRef Medline
67. Lu, Y., Liang, F.-X., and Wang, X. (2014) A synthetic biology approach identifies the mammalian UPR RNA ligase RtcB. *Mol. Cell* **55,** 758–770 CrossRef Medline
68. Nandy, A., Saenz-Méndez, P., Gorman, A. M., Samali, A., and Eriksson, L. A. (2017) Homology model of the human tRNA splicing ligase RtcB. *Proteins.* **85,** 1983–1993 CrossRef Medline
69. Hanson, G., and Coller, J. (2018) Codon optimality, bias and usage in translation and mRNA decay. *Nat. Rev. Mol. Cell Biol.* **19,** 20–30 CrossRef Medline
70. Frabutt, D. A., and Zheng, Y.-H. (2016) Arms race between enveloped viruses and the host ERAD machinery. *Viruses* **8,** 255 CrossRef Medline
71. Russo, J., Heck, A. M., Wilusz, J., and Wilusz, C. J. (2017) Metabolic labeling and recovery of nascent RNA to accurately quantify mRNA stability. *Methods* **120,** 39–48 CrossRef Medline
72. Ford, L. P., Watson, J., Keene, J. D., and Wilusz, J. (1999) ELAV proteins stabilize deadenylated intermediates in a novel *in vitro* mRNA deadenylation/degradation system. *Genes Dev.* **13,** 188–201 CrossRef Medline
73. Sokoloski, K. J., Wilusz, J., and Wilusz, C. J. (2008) The preparation and applications of cytoplasmic extracts from mammalian cells for studying aspects of mRNA decay. *Methods Enzymol.* **448,** 139–163 CrossRef Medline
74. Weger-Lucarelli, J., Duggal, N. K., Bullard-Feibelman, K., Veselinovic, M., Romo, H., Nguyen, C., Rückert, C., Brault, A. C. Bowen, R. A., Stenglein, M., Geiss, B. J., and Ebel, G. D. (2017) Development and characterization of recombinant virus generated from a New World Zika virus infectious clone. *J. Virol.* **91,** 139 CrossRef Medline
75. Lazear, H. M., Govero, J., Smith, A. M., Platt, D. J., Fernandez, E., Miner, J. J., and Diamond, M. S. (2016) A mouse model of Zika virus pathogenesis. *Cell Host Microbe* **19**, 720–730 CrossRef Medline
76. Mukherjee, D., Gao, M., O'Connor, J. P., Raijmakers, R., Pruijn, G., Lutz, C. S., and Wilusz, J. (2002) The mammalian exosome mediates the efficient degradation of mRNAs that contain AU-rich elements. *EMBO J.* **21,** 165–174 CrossRef Medline
77. Soto-Acosta, R., Xie, X., Shan, C., Baker, C. K., Shi, P. Y., Rossi, S. L., Garcia-Blanco, M. A., a Bradrick, S. (2018) Fragile X mental retardation protein is a Zika virus restriction factor that is antagonized by subgenomic flaviviral RNA. *Elife* e39023 CrossRef Medline
78. Picelli, S., Björklund, A. K., Reinius, B., Sagasser, S., Winberg, G., and Sandberg, R. (2014) Tn5 transposase and tagmentation procedures for massively scaled sequencing projects. *Genome Res.* **24,** 2033–2040 CrossRef Medline
79. Neumann, T., Herzog, V A., Muhar, M., von Haeseler, A., Zuber, J., Ameres, S. L., and Rescheneder, P. (2019) Quantification of experimentally induced nucleotide conversions in high-throughput sequencing datasets. *BMC Bioinformatics* **20**, 258 CrossRef Medline